AN EXPERIMENTAL STUDY IN A LARGE FLUME OF HEAVY MINERAL SEGREGATION UNDER ALLUVIAL FLOW CONDITIONS

by

Lawrence L. Brady
B.S., Kansas State University, 1958
M.S., The University of Kansas, 1967

Submitted to the Department of Geology and the Faculty of the Graduate School of the University of Kansas in partial fulfillment of the requirements for the degree of Doctor of Philosophy. 1971

Dissertation Committee:

_____

_____

_____

_____

_____

_____

TABLE OF CONTENTS

LIST OF ILLUSTRATIONS

Figure Page

LIST OF TABLES

ABSTRACT

Segregation of opaque heavy minerals (mainly ilmenite and magnetite) from the light minerals in a natural sand was observed in a large (61 m x 2.44 m x 1.22 m) recirculating water-sediment flume. Bed material (median size .286 mm) used in the study was taken from the Rio Grande near Bernardo, New Mexico. Opaque heavy minerals (median size .144 mm) present in the bed material comprised 0.38 percent of the bed material volume. Significant hydraulic variables, bed configuration, and sorting and bedding patterns of the bed material were observed for four different bed configurations including a flat bed (upper flow regime), a transition bed, and two different dune beds (lower flow regime).

Accumulations of opaque heavy minerals were formed as three basic types including:

1. thin accumulations of opaque heavy minerals covering small areas that were associated with the stoss sides of large dunes with topset beds and with dunes that lacked topset beds;

2. accumulations associated with the topset deposits of large dunes and with dunes formed in the transition flow;

3. accumulations associated with the flat-bed condition.

The most important factors influencing the type and amount of accumulation of opaque heavy minerals are bed configuration and grain density. Sorting of heavy minerals associated with flat beds occurred mainly at the base of the planar beds, where the most widespread deposit of opaque heavy minerals of the three segregating processes form. The thickest deposits of opaque heavy mineral grains are associated with topset deposits of dune beds, but local conditions must be optimum for thick accumulations to occur. Density is important to segregation because the difference in shear stress

necessary to move the light minerals and to move opaque heavy minerals is large. This is shown by means of theoretical considerations of the forces necessary to move grains of two different densities and by means of analysis of the bed material and core samples using Shields criteria for initiation of motion.

Studies of suspended sediment samples from several locations in each run show that the opaque heavy minerals made up less than 0.3 percent by volume of the suspended material. The greater portion of the opaque heavy mineral grains was transported as bed load.

Among measured sediment properties (size, gradation, and shape) of high and low density grains obtained from core samples taken from the bed, significant variations among different runs were observed for the gradations of opaque heavy mineral samples and median sizes of light minerals sampled from laminae adjacent to or within the opaque heavy mineral laminae. Equal fall velocities of grains of the two different mineral groups were determined to have little importance in local segregating mechanisms.

INTRODUCTION

In an alluvial channel, bedding patterns produced in sediment are responses to the different hydraulic variables of a specific flow. Variations in sorting and rates of sorting, or the segregation of the transported materials according to size, shape, and density, are important elements in the producing of bedding structures and in their recognition in sediments and sedimentary rocks.

Relatively little is understood about the local hydraulic conditions or the sediment responses to these conditions that are responsible for sorting of sediments. The relative densities of particles and stream flow characteristics have long been assumed to be important factors in sorting but their relative contribution to the sorting process has not been well understood.

The relationship of heavy minerals to the more common low density minerals was first described in relation to given hydraulic conditions by Rubey (1933). Equal fall velocities of minerals of different densities were considered by Rubey to be the most important factor accounting for the close association of small high density grains with low density but larger mineral grains in a sediment. Other factors considered important by Rubey (1933, p. 3) were density and hardness of the minerals, differences in original sizes of the grains in the source rock, amount of abrasion during transport, and degree of sorting at the site of deposition.

Rittenhouse (1943) used the concept of hydraulic equivalence to explain mineral relations in sands of the Rio Grande in New Mexico. He described hydraulic equivalence (p. 1749) as: ". . . whatever the hydraulic conditions may be that permit the deposition of a grain of particular physical properties, these conditions will also permit deposition of other grains of equivalent value." The distribution of heavy minerals in the stream bed is considered by Rittenhouse (p. 1742-1743) to

be caused by varying hydraulic conditions at the time and place of deposition, equivalent hydraulic size of each of the heavy minerals, availability of the minerals, and unknown factors.

Studies on sorting of minerals with different densities were conducted simultaneously with studies of turbulence, bed resistance and sediment transport by the U. S. Geological Survey at the Engineering Research Center at Colorado State University. Experiments were conducted in a large recirculating sediment flume using natural sand from the Rio Grande south of Albuquerque, New Mexico. As part of the project, this research was undertaken in an effort to find (1) what sediment properties and hydraulic variables are responsible for the rapid segregation of certain heavy minerals in a moving sediment load, and to find (2) the modes by which heavy minerals are transported and deposited after segregation has occurred.

Four flows were studied at near equilibrium conditions. Observations were made of the significant hydraulic variables, sediment transport rate, sediment sorting, and the physical characteristics of the sediments entrained by each flow to obtain the information necessary to explain the sorting processes.

This study contributes to the understanding of local sorting processes that affect grains of different densities. Techniques used and results obtained can be applied to other studies of bedding in modern sediment and in interpretation of ancient sand deposits. Further, observations made in these flume studies of modes of segregation, transport, and accumulation of heavy minerals should help in future research on and exploration for economically valuable placer deposits.

Acknowledgments

Professors W. M. Merrill and E. C. Pogge, University of Kansas, Dr. H. E. Jobson of the U. S. Geological Survey, and Professors M. E. Bickford, A. J. Rowell, and J. D. Winslow, also of the University of Kansas counseled during the research and critically reviewed the manuscript.

The U. S. Geological Survey permitted access to the flume and laboratory facilities at the Engineering Research Center at Colorado State University, Fort Collins, Colorado. The U. S. Geological Survey staff, especially Drs. R. S. McQuivey, R. E. Rathbun, H. E. Jobson, V. R. Schneider, and J. P. Bennett, furnished aid during flume runs and discussion of data during its analysis. In addition, Dr. C. F. Nordin, and Messrs. H. P. Guy, D. R. Dawdy, of the U. S. Geological Survey staff, Dr. N. S. Grigg, and Messrs. R. C. Olsen, T. N. Keefer, M. R. Karlinger, and Baum-Loo Lee, part-time staff members, assisted during various stages of the study.

Professors E. V. Richardson and D. B. Simons of Colorado State University and Dr. W. P. Albrecht, Dean of Graduate School, University of Kansas, worked out administrative arrangements between Colorado State University, the U. S. Geological Survey, and the University of Kansas, that led to the use of facilities necessary for this study.

THEORETICAL CONSIDERATIONS

Relative Velocities of Water Transported Particles with Differing Densities

Consideration of the forces acting on discrete particles in a few idealized situations can provide an approximation of conditions in the natural environment. Actual values for the velocities and forces involved in the grain movement would be very difficult to determine experimentally. However, by making certain assumptions deduced for grains with different densities approximate relative velocities of grains can be developed.

For immersed particles moving along a bed, five principal forces are important in determining the movement of the particle. These forces include the (1) gravity forces related to the immersed weight of particles, the (2) drag and (3) lift forces that result from pressure and frictional effects of the fluid on the particles, (4) frictional forces that result from contact between the grains and bed, and (5) forces resulting from adjacent moving grains.

By considering an individual spheres that move without interference from adjacent moving grains, the principal forces[1] can be defined as

1. Gravity Force

$$F_G = \frac{\pi d^3}{6}(\rho_s - \rho)g \qquad (1)$$

2. Hydrodynamic Drag

$$F_D = C_D A_s \rho \frac{V_o^2}{2} = C_D \frac{\pi d^2}{8} \rho (V_f - V_s)^2 \qquad (2)$$

---

[1]For further explanation of drag and lift forces (equations 2 and 3) acting on a body, refer to a standard fluid mechanics text (e.g. Daily and Harleman, 1966, p. 170-171). Frictional force relations (equation 4) are further explained in Sears and Zemansky (1963, p. 35), and other basic physics or mechanics texts. The gravity force (equation 1) is the resultant force acting on the particle that is dependent on the immersed weight of the particle and the gravitational constant.

3. Hydrodynamic Lift

$$F_L = C_L A_s \rho \frac{V_o^2}{2} = C_L \frac{\pi d^2}{8} \rho (V_f - V_s)^2 \quad (3)$$

4. Friction Force

$$F_F = C_F F_N = C_F (F_G \cos \emptyset - F_L) \quad (4)$$

in which

A_s = is the projected area of the sphere normal to the flow
C_D = coefficient of drag
C_L = coefficient of lift
C_F = coefficient of kinetic friction between the particle and the bed
d = diameter of the sphere
F_F = frictional force
F_G = force of gravity
F_D = drag force
F_L = lift force
F_N = forces normal to the contact surface exerted by the particle
g = gravitational constant (980 cm/sec^2)
V_f = velocity of flow at a representative distance above the bed
V_o = relative velocity of flow past a body
V_s = velocity of translation of the particle
$\emptyset$ = angle between the bed surface and horizontal. A positive value indicates that the bed surface is rising in a downstream direction such as on the upstream side of a ripple or dune.
ρ = mass density of fluid
ρ_s = mass density of particle

(For further explanation of symbols, see Appendix A). The four forces as applied to a spherical particle are shown schematically in figure 1.

Value of the gravity force is dependent on the immersed weight of the particle and the gravitational constant (980.7 cm/sec^2). Gravitational forces can either oppose or supplement drag forces depending on the sine of $\emptyset$ (fig. 1). Frictional forces acting on moving particles are difficult to determine. For purposes of this study the frictional force was assumed proportional to the normal force between the particle and the bed. The constant of proportionality is the coefficient of kinetic friction.

Hydrodynamic drag on a grain is dependent on the frictional drag resulting from surface shear between the grain and the fluid, and the shape of the grain or form resistance, which results from pressure drag

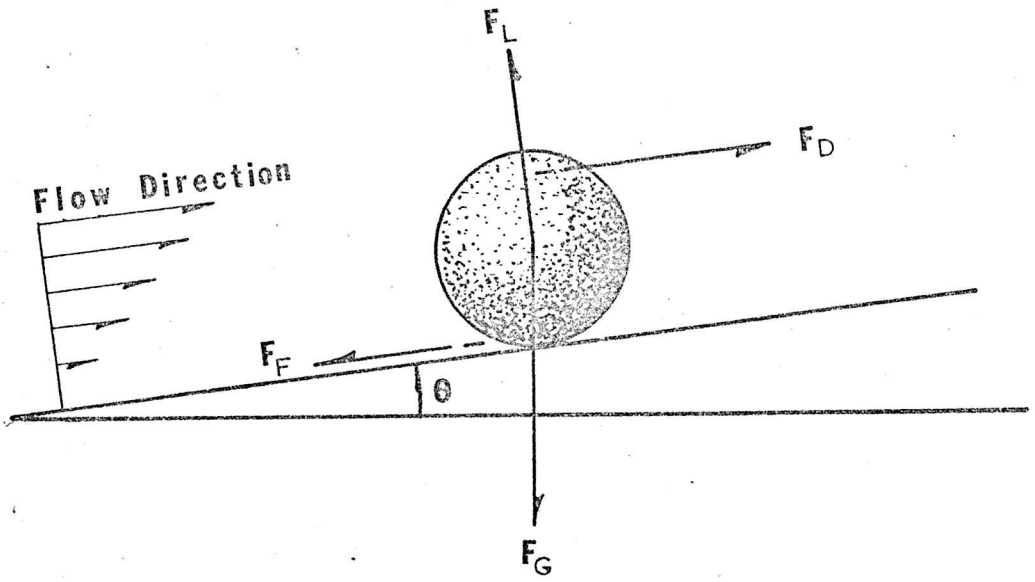

Fig. 1. Schematic diagram of forces acting on a discrete moving particle in a fluid.

on the particle. It is customary to define a total drag coefficient C_D to include both frictional and form drag.

Lift forces produced on a body are due primarily to a difference in pressure between the upper and lower sides of the particle. Increased velocity resulting from fluid acceleration around the upper side of a grain causes a local reduction in pressure, while the pressure on the lower side of the grain surface at or near the bed approaches the static pressure of the fluid.

The fluid velocity, V_f , in equations (2) and (3) refers to the fluid velocity at some representative distance above the bed.

By use of the four fundamental equations (1 through 4), a general motion equation for particles can be ~~established~~ derived. Direct comparisons between grains or different densities can then the made by establishing ratios of their translating motion of the grains of greater density to that of the grains of lesser density and reducing the equations to a form that expresses the relative difference in the velocities of the two grain types for the same flow conditions.

For a particle in motion and having a uniform velocity, the general translation motion equation for the particle can be expressed as

$$F_F = F_D - F_G \sin \theta \tag{5}$$

By dividing the frictional force on one particle by the frictional force on a particle of different density, the following ratio can be established using equations (4) and (5).

$$\frac{F_F}{F_{F_1}} = \frac{F_D - F_G \sin \theta}{F_{D_1} - F_{G_1} \sin \theta} = \frac{C_F (F_G \cos \theta - F_L)}{C_{F_1} (F_{G_1} \cos \theta - F_{L_1})} . \tag{6}$$

The subscript (1) is used to denote the forces and coefficients affecting the sphere of the lower density.

By substituting equations (1) to (3) into equation (6), and simplifying terms, the following equation can be developed.

$$\frac{C_D \rho 3 (V_f - V_s)^2 - 4 d g (\rho_s - \rho) \sin \theta}{C_{D_1} \rho 3 (V_{f_1} - V_{s_1})^2 - 4 d_1 g (\rho_{s_1} - \rho) \sin \theta} =$$

$$\frac{C_F [4 d g (\rho_s - \rho) \cos \theta - 3 C_L \rho (V_f - V_s)^2]}{C_{F_1} [4 d_1 g (\rho_{s_1} - \rho) \cos \theta - 3 C_{L_1} \rho (V_{f_1} - V_s)^2]} . \qquad (7)$$

By considering $\phi = 0$ equation (7) can be simplified to

$$\frac{C_D (V_f - V_s)^2}{C_{D_1} (V_{f_1} - V_{s_1})^2} = \frac{C_F [4 d g (\rho_s - \rho) - 3 C_L \rho (V_f - V_s)^2]}{C_{F_1} [4 d g (\rho_{s_1} - \rho) - 3 C_{L_1} \rho (V_{f_1} - V_{s_1})^2]} . \qquad (8)$$

Equation (8) can be used to determine the relative velocities of rolling spheres with different densities.

Assuming the two spheres have equal diameters and therefore equal drag coefficients and equal lift coefficients and assuming equal coefficients of friction, equation (8) reduces to

$$\frac{(V_f - V_s)^2}{(V_f - V_{s_1})^2} = \frac{(\rho_s - \rho)}{(\rho_{s_1} - \rho)} . \qquad (9)$$

By applying densities of materials of interest in this study: 5.0 g/cm^3 for ρ_s, 2.65 g/cm^3 for ρ_{s_1}, and 1.0 gm/cm^3 for ρ, equation (9) can be expressed in dimensionless form as

$$\frac{V_s}{V_{s_1}} = 1.56 - \left(\frac{1.79 V_{s_1}}{V_f} \right)^{-1} \qquad (10)$$

A graph of equation 10 is shown in figure 2.

The relative velocities of spheres of the two different densities are clearly shown in figure 2. The velocity of the denser sphere (V_s) is always less than that of the lighter sphere (V_{s_1}) except where both are equal to the fluid velocity (V_f), a condition where there is no frictional

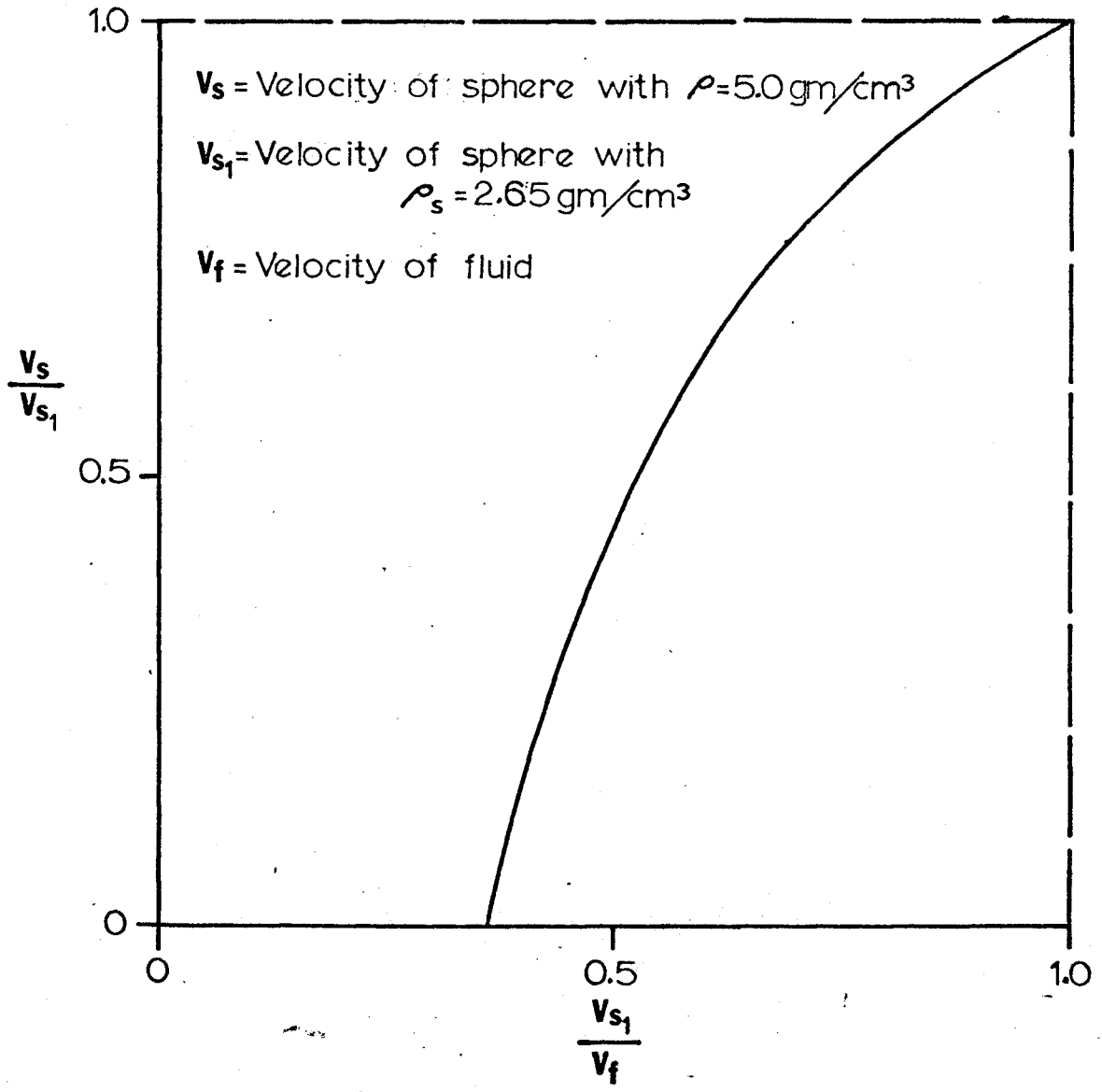

Fig. 2. Velocity ratios of equal size spheres but with different densities.

force. This condition could occur when both particles are suspended. As the velocity of the lighter particle becomes progressively smaller, the relation $\frac{V_s}{V_{s_1}}$ also becomes progressively smaller until a point is reached where movement of the denser sphere ceases. At this point—the point of incipient motion of the denser particle—the light density particle is moving at a relatively rapid rate.

A second situation that can be approximated is that of two spherical particles of equal submerged weight but having different densities. Substituting values for the densities of the spherical particles of 5.0 g/cm^3 and 2.65 g/cm^3, the ratio of diameters required to obtain equal submerged weight is 1:1.34. Additional conditions, however, must be assumed ~~imposed~~ in order to derive a general velocity formula such as equation (10).

1. For consideration in the drag force equation, a drag coefficient ratio (C_D / C_{D_1}) of 1.2:1 is assumed. Drag coefficients of the two spheres will differ because of their difference in size. The value of 1.2:1 was approximated from the C_D vs. Re diagram in the U. S. Inter-Agency Committee on Water Resources Report 12 (1957, p. 20) by using grain sizes similar to the experimental runs (.12mm for the high density grain and .163 mm for the low density grains). Here Re refers to the Reynolds number relative to a particle.

2. The lift forces for this situation are ignored. In an experimental situation a small amount of lift should be present for a particle near the bed, but lift forces are ignored here because of the complications they would impose on the derivation.

3. The coefficient of friction is considered to be same for both spherical particles. This value in reality, would probably be different for each sphere because the statistical mean of the angles between the point of

contact of stationary particles on the bed projected through the center of the moving sphere and a line normal to the bed would be larger for the sphere of a smaller radius ($C_f > C_{f_1}$).

4. An assumption is made for this analysis that the increase in fluid velocity is linear, as it is in the laminar sublayer, at least up to a point where the characteristic velocity is determined, and the fluid velocity is at the bed surface. For two spheres the diameters of which are in the ratio of 1:1.34, the fluid velocity at the point of drag force application of the small sphere would be .746 of the value of the fluid velocity at the corresponding point on the larger sphere.

Accepting assumptions ~~Under~~ these ~~additional conditions~~, the basic equation (8) can be reduced to

$$\frac{V_s}{V_{s_1}} = 1.22 - \left(\frac{2.09\, V_{s_1}}{V_f}\right)^{-1} \qquad (11)$$

Figure 3 represents a plot of equation (11) for relevant particle velocities.

For the development of equations (8), (10), and (11), the bed surface was considered horizontal; but relations shown in figures 2 and 3 should be qualitatively similar for any given bed form slope. The basic difference in forces when considering slope is the effect of grain weight on the grain movement.

A gravity force component parallel to the bed will act against the drag force if the local bed surface is inclined in a direction opposite to the energy slope or the stream gradient. This condition is analogous to grain movement up the stoss side of a dune or ripple (fig. 1). When the local bed surface is inclined in the direction of the energy slope or stream gradient such as occurs on a flat bed or the lee slope of a dune,

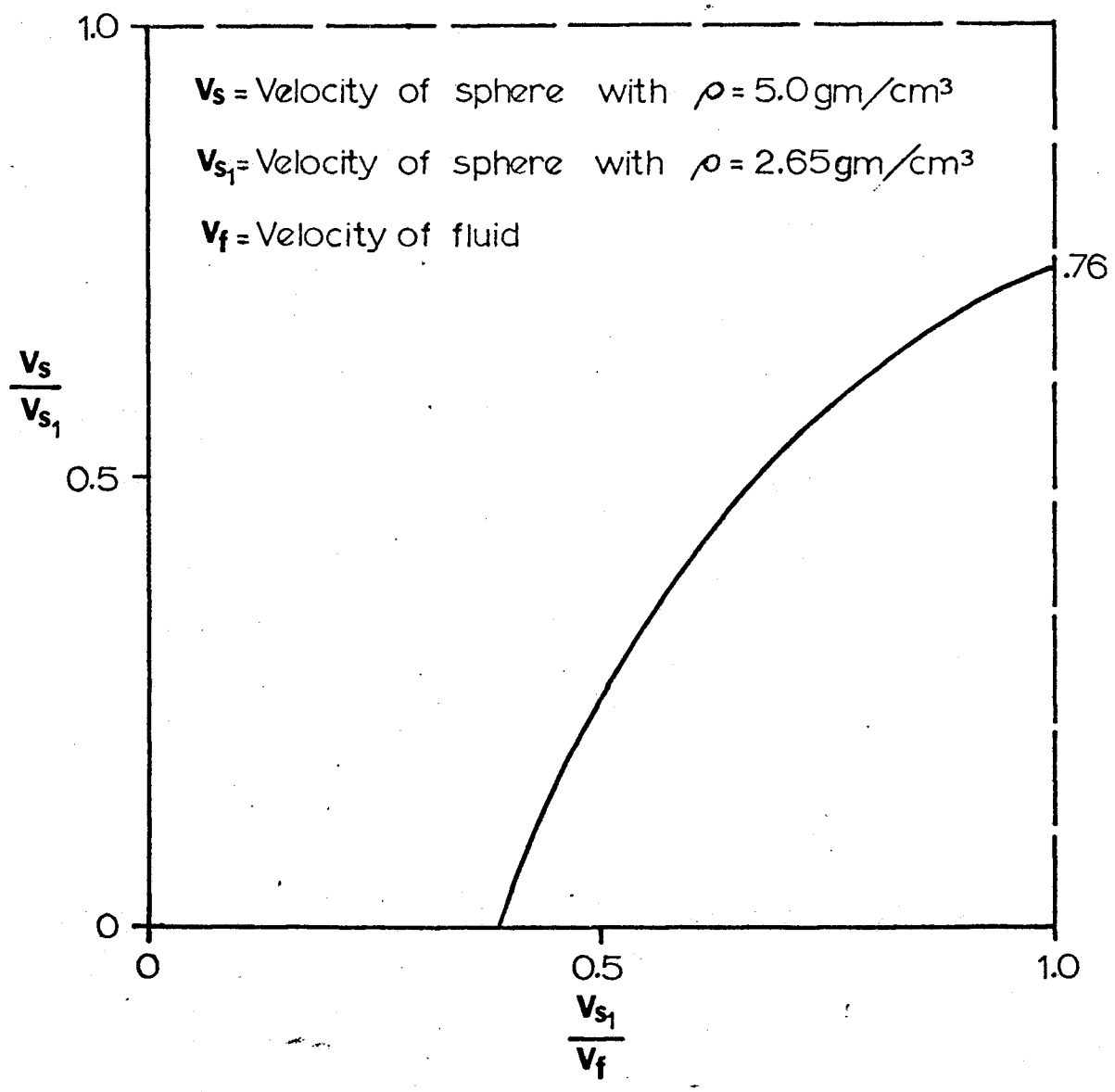

Fig. 3. Velocity ratios of spheres of equal submerged weight but having different densities.

the particle weight then becomes additive to the drag force in influencing grain movement downstream.

In addition to the effect of gravity, frictional forces resulting from differences in the bed surface will have a marked effect on the grain velocity. A coarse sand bed would provide a higher coefficient of friction than a finer sand bed for a given grain size in movement.

Grains moving at the surface of a sediment bed are continually being deposited and re-entrained at a rate dependent on the local conditions of the flow. When considering velocities for high and low density grains that are much lower than the fluid velocity, there exists a large difference between the velocities of the two grain types (fig. 2 and 3). It is at this stage where large differences in the velocities of the two types of grains exist or under conditions prior to movement of high density grains, that sorting of the two grain types is most likely to occur. The low density grains can be entrained and moved much more readily than the high density grains and during transport the high density grains would be deposited first. This type of situation would provide for efficient sorting by accumulating high density grains in areas where the flow is not readily capable of transporting the grains while the low density grains are rapidly transported past the area.

These considerations show in a simplified manner that small dense grains are more resistant to surface movement than are larger low density grains. Graphs similar to figures 2 and 3 can be constructed for natural materials of any density. Then, by considering realistic conditions as observed in sediments in the natural alluvial environment, the graphs can help explain some of the observed bedding features that involve materials of different densities.

Shear Stress as a Density Sorting Parameter

Consideration of critical shear stress (τ_c), the stress exerted by the flow on the bed that is just capable of initiating grain movement, adds insight into the sorting of grains of varying densities. Shields (1936) plotted experimental results of the beginning of particle motion based on a dimensionless shear stress (τ_*) and a particle Reynolds number (R_*) where

$$\tau_* = \frac{\tau_c}{(\gamma_s - \gamma) d_s}$$

and

$$R_* = \frac{U_* d_s}{\nu}$$

with γ_s equal to the specific weight of the sediment grains, γ the specific weight of the fluid, d_s the grain diameter, U_* is the shear velocity or $\sqrt{\tau_o/\rho}$ with ρ the fluid density, ν is the kinematic viscosity of the fluid, and τ_o is the average shear stress at the bed.

Additional data and refinement of this plot by later workers has resulted in the generally accepted Shields diagram shown in figure 4 (A.S.C.E. Task Committee on Preparation of Sedimentation Manual, 1966, p. 297). Based on the curve (fig. 4), one can develop the relation of critical shear to grain size for grains of different densities. Grigg and Rathbun (1969) have developed such a series of curves that show on a theoretical basis, that grains of different density but equal fall velocity require different shear stress for initiation of movement. For a grain diameter below 0.1 mm, Grigg and Rathbun (1969, p. 79) show that critical shear is a function only of grain density, but with grains larger than 0.1 mm the critical shear becomes a function of size as well as density.

Conditions under which the Shields diagram was developed were quite different from conditions that existed during the four flume runs. Data used to develop the Shields curve were obtained from artifically flattened

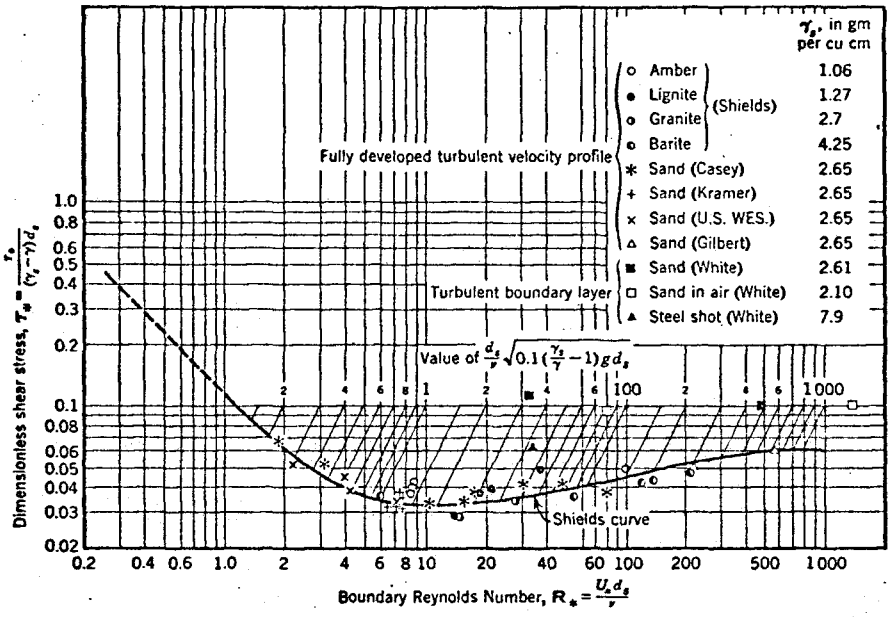

Fig. 4. Shields diagram showing sediment entrainment as a function of the particle Reynolds number. (Taken from the A.S.C.E. Task Committee on Preparation of Sedimentation Manual, 1966, p. 297)

sand surfaces with uniform size grains under fully developed turbulent flows in which shear at the bed was just large enough to initiate a few grain movements. In contrast to conditions at initiation of sediment motion, large amounts of sediment are in transport at relatively high velocities on stream beds when sorting occurs during the experimental runs.

Even though Shields' (1936) work was developed for the situation of very small amounts of sediment motion, it gives insight into relations among moving grains because during a given flow grains are continually being deposited and then reentrained into the flow. One can see, at least qualitatively, from Shields' work that the denser grains will require a much larger shear stress for movement than lighter grains.

An extension of the threshold of motion considerations is the problem of determining the quantity of sediment in transport by grains rolling or sliding along the bed surface. Best known among the bed-load equations is the Einstein bed-load function (Einstein, 1950). Einstein's bed-load equations express a relation between the intensity of shear on a particle (ψ) and intensity of transport (ϕ) where

$$\Phi = \frac{q_B}{\gamma_s}\left(\frac{\gamma}{\gamma_s-\gamma}\,\frac{1}{g d_s^3}\right)^{\frac{1}{2}}$$

and

$$\psi = \frac{\gamma_s-\gamma}{\gamma}\,\frac{d_s}{R'S}$$

where q_B is the rate of transport of the bed-load in weight of total bed load per time and width, g is the gravitational constant, d is the grain diameter, S is the energy slope and R' is the hydraulic radius with respect to the particles (if all resistance to flow is due to particle resistance and none due to the bed or stream bank configuration). The shear intensity

parameter (ψ) of Einstein is essentially the reciprocal of Shields dimensionless shear stress (τ_*) and is important in determining the amount of total transport rate of the bed load (q_s).

Bed Forms Produced by Flow in an Alluvial Channel

Shortly following initiation of movement of the bed material, bed forms start to develop. These initial forms are described by Kennedy (1963, p. 522) as ". . . the result of scour and deposition due to the perturbation velocities induced by any protuberance on the bed." Flows in alluvial channels are classified into two flow regimes (upper and lower) with a transition zone between that are based on the bed configuration, mode of sediment transport, process of energy dissipation, and phase relation between the bed and water surfaces (Simons and Richardson, 1963). Relationships of bed forms within these two regimes are shown in table 1 and figure 5.

The A.S.C.E. Task Force on Bed Forms in Alluvial Channels (1966, p. 53) defines ripples as bed forms with wave lengths less than approximately one foot and heights less than 0.1 foot. Dunes are bed forms larger than ripples and out of phase with any water-surface gravity waves that accompany them, while a flat bed is a bed surface devoid of bed form. Antidunes and chutes-and-pools are in the upper portion of the upper flow regime but were not studied in this series of experiments (these features are described by Simons, Richardson, and Nordin, 1965, p. 40-42).

Bed forms within the lower flow regime include ripples, ripples superimposed on dunes, and dunes. In the lower regime the water surface waves and undulations are out of phase with the bed undulations. In general, resistance to flow is high while sediment transport is small. In natural streams, dunes or dunes with superimposed ripples are the most common bed forms (Simons and Richardson, 1966, p. 11).

Table 1.—Classification of flow regimes (Adapted from Simons, Richardson, and Nordin, 1965, p. 36)

Flow regime	Bed form	Bed Material concentrations (ppm)	Mode of sediment transport	Type of roughness	Phase relation between bed and water surface
Lower regime	Ripples	10–200	Discrete steps	Form roughness predominates	Out of phase
	Ripples on dunes	100–1,200			
	Dunes	200–2,000			
Transition	Washed out dunes	1,000–3,000		Variable	
Upper regime	Plane beds	2,000–6,000	Continuous	Grain roughness predominates	In phase
	Antidunes	2,000→			
	Chutes and pools	2,000→			

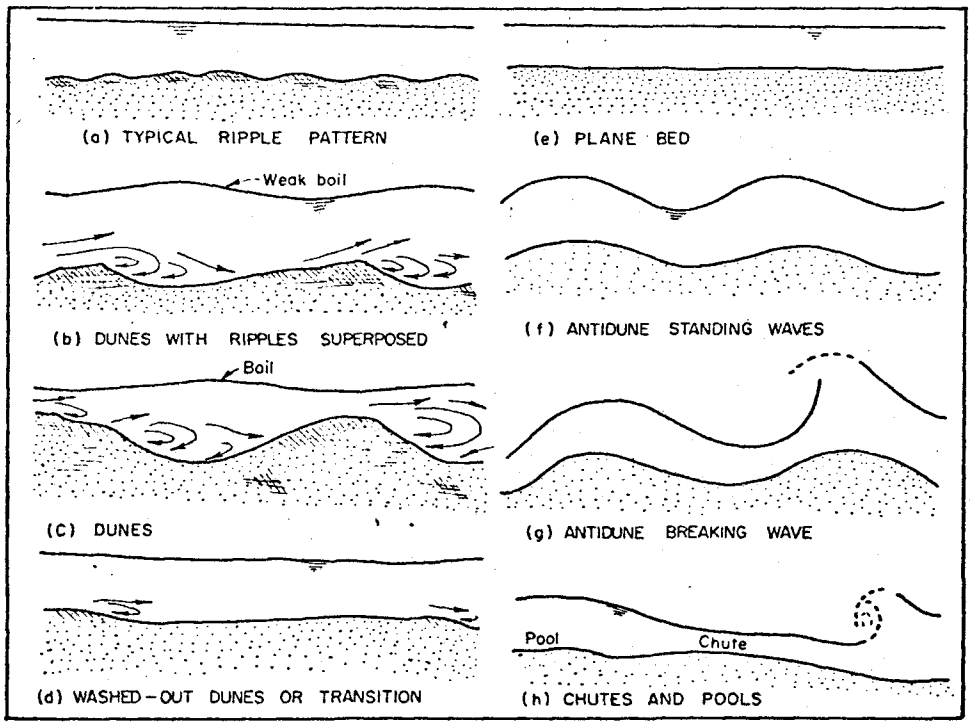

Fig. 5. Idealized diagram of bed forms in an alluvial channel. (Taken from Simons, Richardson, and Nordin, 1965, p. 36)

Within the transition flow the bed configuration is very erratic and may include forms common to both the upper and lower regimes. Dunes present in the transition zone will often decrease in amplitude and increase in length before the bed becomes plane (washed-out dunes) (Simons and Richardson, 1966, p. 11).

In the upper flow regime the usual bed forms are flat beds (plane beds) or antidunes, with small resistance to flow and large sediment transport. Water surface waves in this regime are in phase with the bed surface except during the breaking of an antidune (Simons and Richardson, 1966, p. 11).

Bed forms produced by the four different experimental runs in this study were dunes in the lower flow regime, long profile dunes in the transition zone, and a flat bed in the upper flow regime. Terminology used in this report for the different surface features of dunes, and the bedding structures associated with the dunes, is shown in figure 6.

Relation of Grain Entrainment to Turbulence

The effect of turbulence in a given flow is an important factor in grain entrainment. Local boundary shear stress must be determined from the velocity gradient at the bed and cannot be determined from the slope-depth relationship alone. The apparent shear stress (τ) in turbulent flow is expressed by Streeter (1966, p. 226) as

$$\tau = (\mu + \eta)\frac{du}{dy}$$

in which μ is the dynamic viscosity, η is the eddy viscosity that depends on the state of the turbulent motion, and dU/dY is the velocity gradient normal to the bed. Intensity of turbulence is important because high turbulent intensities are indicative of large velocity fluctuations and usually indicate large velocity gradients.

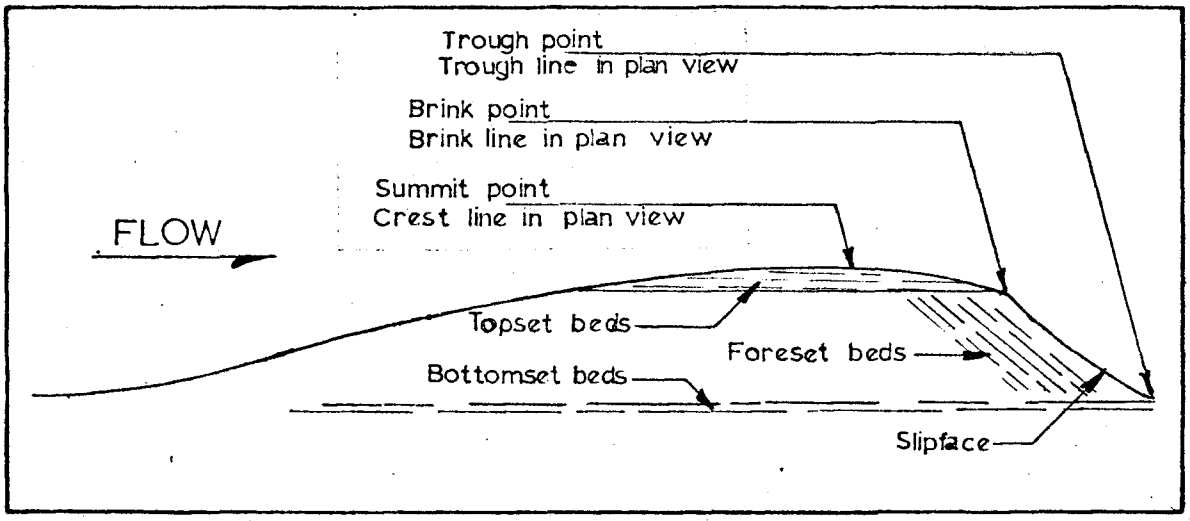

Fig. 6. Dune profile showing terminology used in report (4x vertical exaggeration). Location terminology adapted from Allen, 1968, p.62.

McQuivey and Keefer (1969) studied the segregation of magnetite grains from quartz on the stoss side of ripples in a small flume. Differences in turbulent shear stress from ripple trough to crest and differences in shear stress required for movement of grains of different densities were considered by McQuivey and Keefer as being important factors in heavy mineral segregation. Turbulence measurements using a hot-film anemometer were made over sand ripples by McQuivey and Keefer (1969, p. 246-247), and their results show much larger turbulent intensities over the trough area than over the crestal region of a ripple. Turbulent intensity also decreased with distance from the bed.

Similar results of turbulence measurements are described by Raudkivi (1967, p. 206-207) for experiments conducted by Sheen (1964). Raudkivi describes the greatest turbulent intensities as occurring just downstream from the point of separation (brink line) on a ripple. ~~The most~~ Intense turbulence is present in the trough area with rapidly decreasing turbulent intensities downstream.

R. S. McQuivey of the U. S. Geological Survey (personal communication) (~~report of data in preparation for U. S. Geological Survey Professional Paper~~) made velocity and turbulence measurements at selected locations on the center line for each of the runs in this study. Velocity measurements were made with a modified Ott velocity meter, and turbulence measurements were taken with a constant-temperature hot-film anemometer system using techniques described by Richardson and McQuivey (1968). Results of these studies (fig. 7, 8, and 9) show large turbulent intensity near the bed and much larger turbulent intensities in the trough region than on the dune back or at the brink point. Turbulent intensities are less at the brink point than on the dune stoss side, midway between the dune brink point and the reattachment point of the flow (the location where the flow impedes on the bed after it had passed over the upstream dune front).

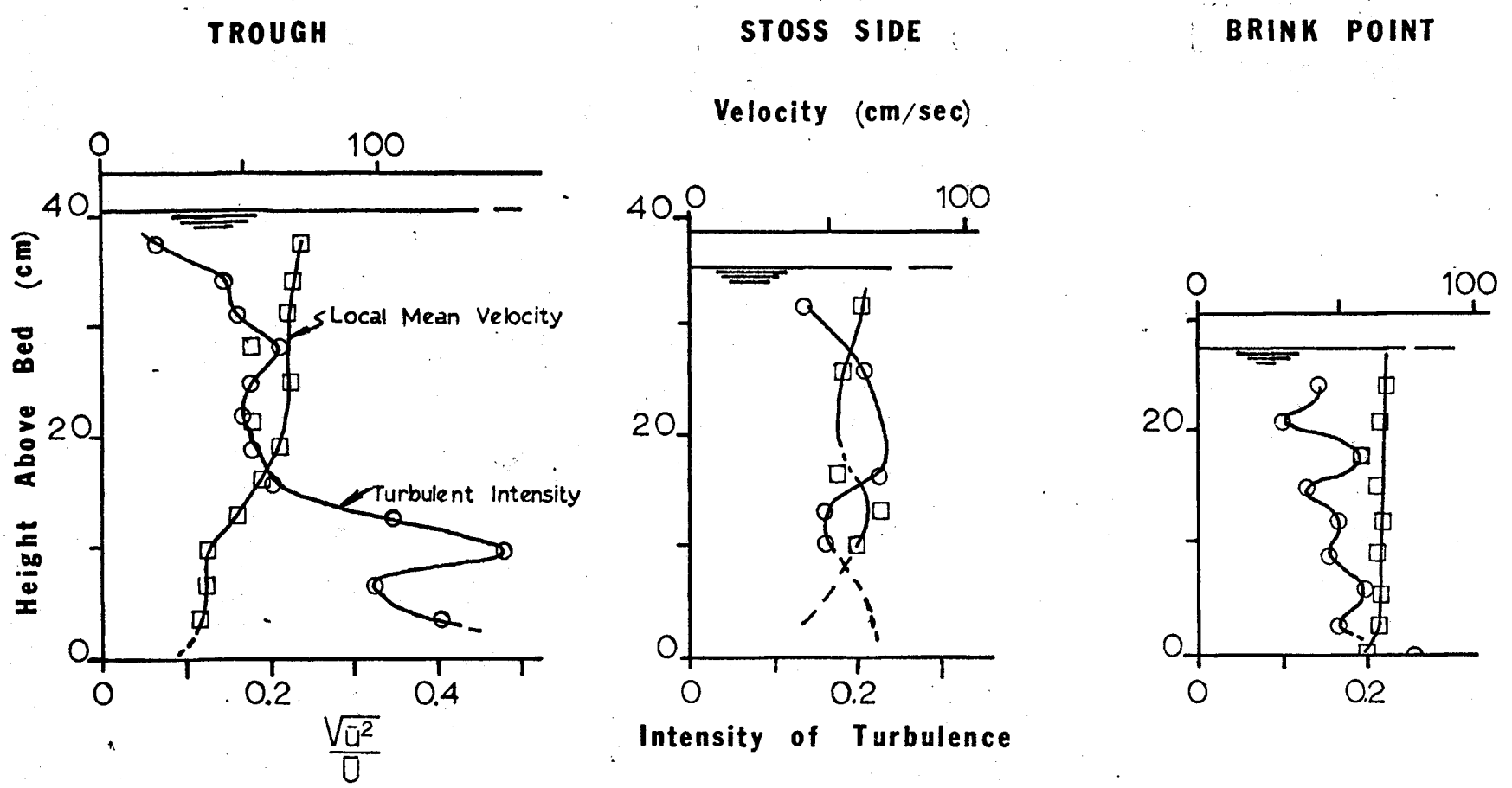

Fig. 7. ~~Run 1:~~ Vertical distribution of local mean velocity and longitudinal turbulent intensity for run 1. (root-mean-square of the longitudinal velocity fluctuations ($\sqrt{\bar{u}^2}$) divided by the local mean velocity ($\bar{U}$)).

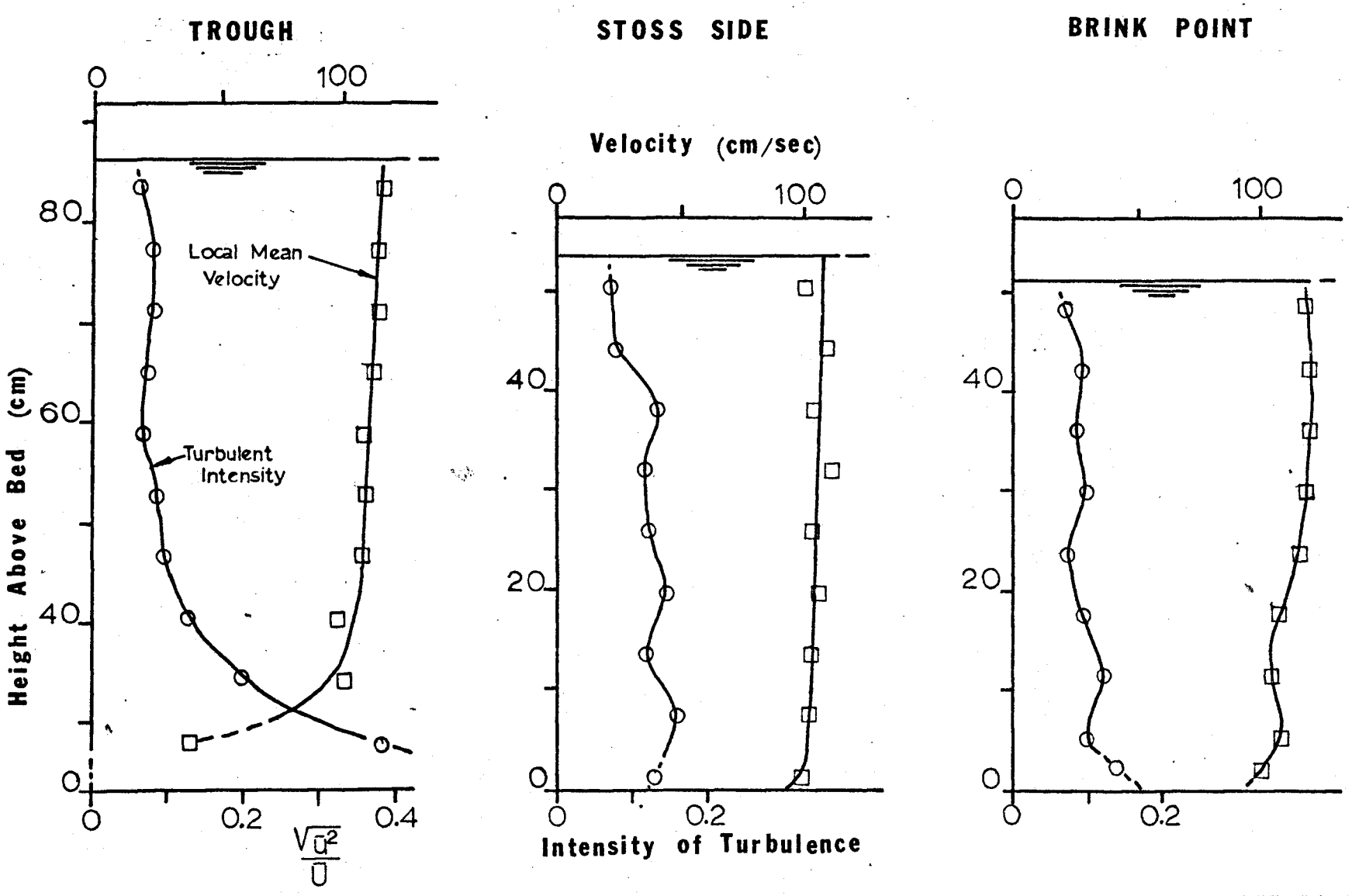

Fig. 8. Vertical distribution of local mean velocity and longitudinal turbulent intensity for run 2.

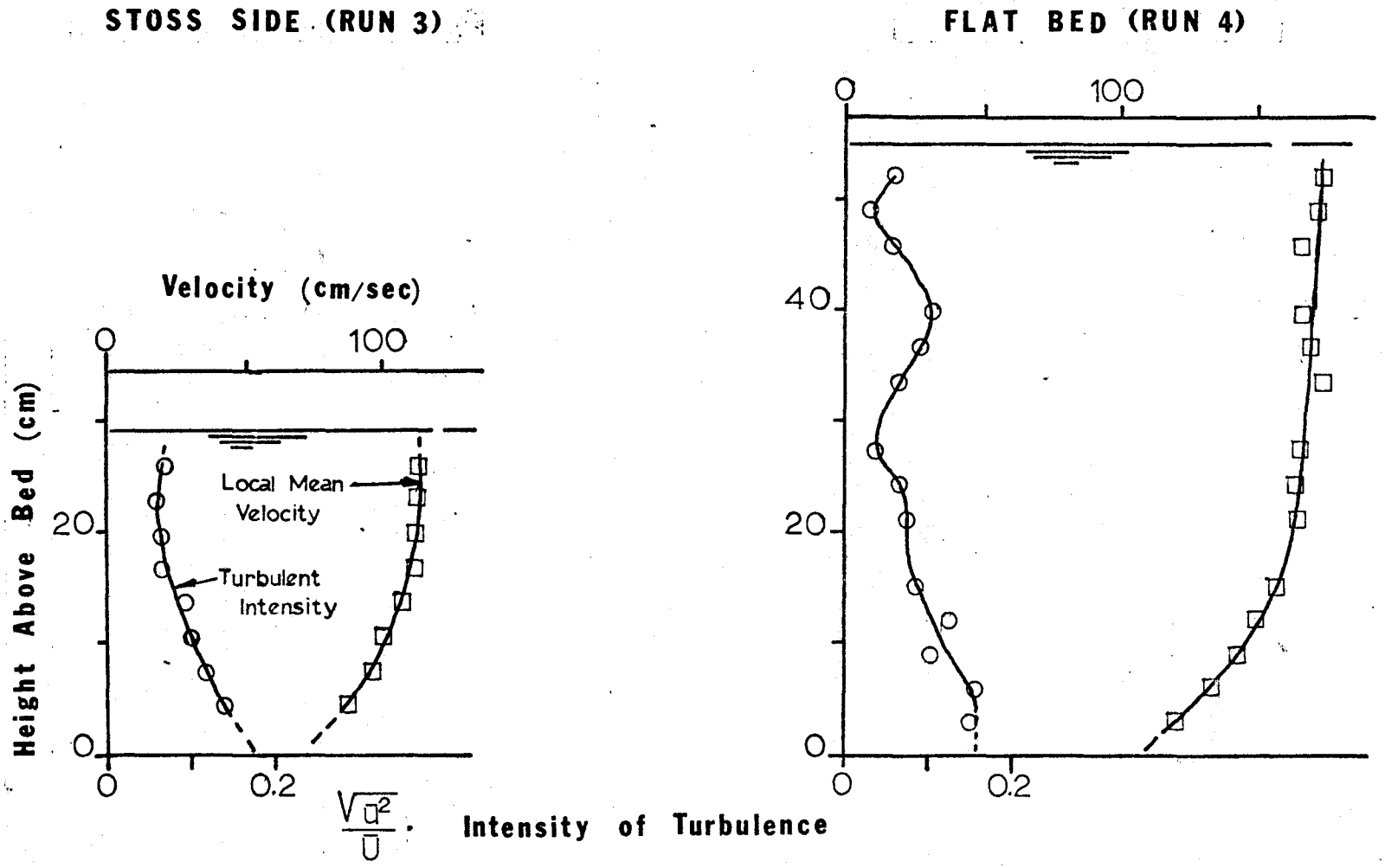

Fig. 9. ~~R~~ Vertical distribution of local mean velocity and longitudinal turbulent intensity for runs 3 and 4.

Summary

Theoretical considerations of grains with different densities lead to the conclusions that: (1) small dense grains are more resistant to tractive movement than larger low density grains; (2) high density grains require much larger shear stress for movement than is required for low density grains; and (3) the shear intensity (Ψ) of Einstein (1950) indicates that boundary shear is an important parameter in determining the rate of sediment transport.

Different bed forms are produced under different flow conditions with ripples and dunes formed in the lower flow regime, flat beds formed in an upper flow regime, and long profile dunes formed under transition flow conditions.

Turbulent intensities of the flows are large near the bed and decrease with distance from the bed. Much larger turbulent intensities occur in the trough regions of dune beds than occur on the crestal areas with the turbulent intensities decreasing rapidly downstream from the trough area toward the brink line of a dune. Intensity of turbulence is important because high turbulent intensities are indicative of large velocity fluctuations and usually indicate large velocity gradients. The amount of local boundary shear stress is dependent on the local velocity gradient.

MATERIALS AND EXPERIMENTAL CONDITIONS

A large recirculating water-sediment flume of rectangular cross-section and dimensions of 61 meters in length, 2.44 meters in width, and 1.22 meters in depth was used for the series of four experiments (fig. 10). The large size of the flume permits the establishment of flow conditions that approximate flow conditions in a natural channel and eliminates many of the boundary effects that are associated with smaller flumes. The slope of the flume can be changed by use of adjustable screw jacks, and water-sediment discharge can be varied up to approximately 2.1 cubic meters per second. The interior of the flume is surfaced with aluminum having an epoxy coating. A transparent plexiglass section 21.95 meters long is located midway along the left wall of the flume that allows observations to be made of sediment movement.

Hydraulic Measurements

Near equilibrium conditions were established for each of the flows before sediment and hydraulic data were taken. After equilibrium flow[2] was established for a given experiment, measurements were made of sediment discharge, water-sediment discharge, slope of the water surface and energy grade line, depth, and water temperature. Additional hydraulic parameters can be calculated from these basic data. Mean values of significant hydraulic variables are shown in table 2.

Water surface elevations for several profiles were measured every 1.52 meters along the center line of the flume. For each profile a line was fitted to the water surface elevation measurements and their

---

[2]Equilibrium flow is defined as flow that has established a bed configuration and slope consistent with the fluid, flow, and bed-material characteristics over the working reach of the bed (Simons and Richardson, 1966, p. 3).

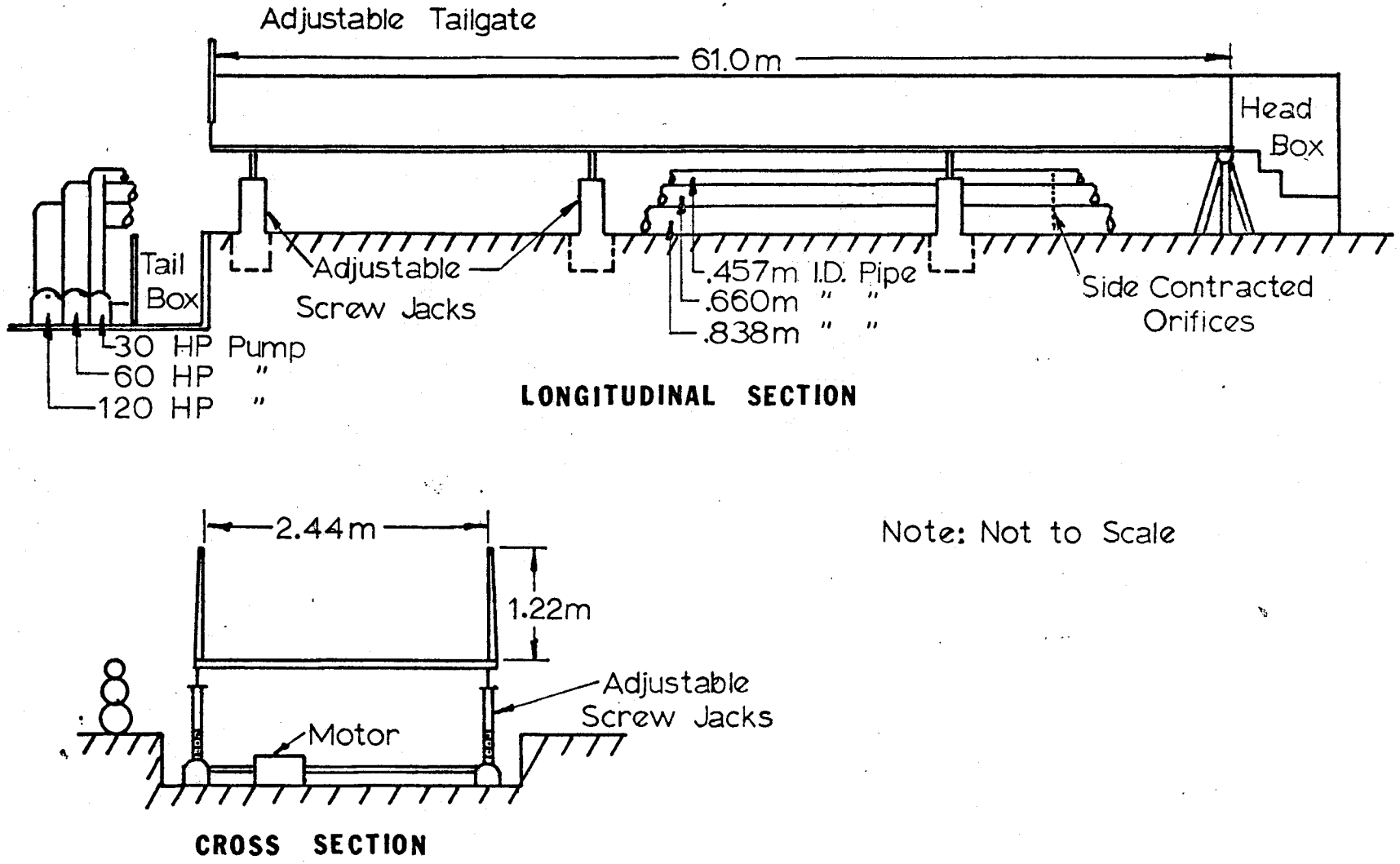

Fig. 10. Schematic diagram of the flume used in the four experimental runs. (Modified from Loyacano, 1967, p. 41)

Table 2--Values of experimental variables and parameters for the four ~~hydraulic~~ flows.

Run	Bed Form	Energy Slope ($\times 10^{-3}$)	Mean Depth (cm)	Water Discharge (cu meters/sec)	Temp. (°C)	Mean Velocity (cm/sec)	Shear stress ($dynes/cm^2$)	Froude Number
1	Dunes	1.0229	32.9	0.4820	20.8	60.0	33.3	0.34
2	Dunes	1.0561	58.5	1.3776	20.9	96.6	60.8	0.40
3	Transition	1.2207	33.7	0.7309	20.7	88.7	40.2	0.49
4	Flat bed	1.7910	52.8	2.0765	21.0	161.2	93.2	0.71

corresponding flume stations by the method of least squares. The mean value of the calculated slopes was taken to be the average water-surface slope for each run. By adding the local velocity head, $\frac{Q^2}{2g(WD)^2}$, where Q is discharge, W is channel width, D is water depth, and g is the gravitational constant, to the water-surface elevation at a given measurement point, the elevation of the energy grade line was obtained. Using the energy line elevation point, the slope of the energy line was determined in a similar manner as the slope of the water surface.

Profiles of the bed and water surfaces along the flume center line were recorded on chart paper by use of a sonic sounder; and from these sounder profiles, the depth of flow was determined. The mean depth of flow (table 2) for the run was determined by averaging the depth values obtained every 1.52 mm along each profile.

Water discharge was determined by use of water-air monometers that were connected to calibrated orifice meters located in the three return-flow pipes. Mean discharge for each run was determined from an average of 4 to 20 individual readings. Water temperature was held as constant as possible by use of steam and cold water. The temperature for each run had a fluctuation of less than $\pm$ 1° C.

Mean velocity ($\overline{U}$) was calculated by use of the continuity equation

$$\overline{U} = \frac{Q}{A} = \frac{Q}{D \times W} .$$

Any error in the mean velocity reported would be primarily due to an error in mean depth readings.

The shear stress at the bed (τ_o) and Froude number (F) are both calculated from the above measured variables. The shear stress is a measure of the resistance to flow of sediment at the bed and is defined for a large area as $\tau_o = \gamma DS$

where γ is specific weight of water and S is the energy slope. The Froude number value is a measure of the effect of gravity on the flow pattern and is defined as

$$F = \frac{U}{\sqrt{gD}}.$$

For a Froude number less than one a flow is defined as tranquil because the average velocity of the flow is less than the velocity of propagation in the fluid of small surface waves. For a Froude number greater than one, the flow is defined as rapid, for the fluid velocity exceeds the velocity of movement of the small surface waves.

Sediment Analysis

Sediment Characteristics--Sand used in the experiments was obtained from a conveyance channel of the Rio Grande near Bernardo, New Mexico. An arkosic sand, it contains approximately 60% quartz, 36% feldspars, 3% rock fragments, and 1% accessory minerals. Heavy minerals within the bed material comprise 1.13% by weight and 0.72% by volume of the total bed-material sample. Dark opaque grains, mainly ilmenite and magnetite, amount to 0.38% of the bed-material sample by volume. In addition to magnetite and ilmenite, there are amphiboles, pyroxenes, garnet, zircon, tourmaline, and hydrous iron oxides.

Within this report classification of the sediments will be divided into opaque heavy minerals consisting of ilmenite and magnetite, and light minerals which comprise the remainder of the mineral grains. These two groupings provided for maximum efficiency in recognition and description of the segregation characteristics and conditions.

Size Analysis - Total Bed Material--Samples for the bed-material analyses (fig. 11) were obtained from a composite sample of ten vertical cores of the bed. Samples were taken at random locations in the flume after the

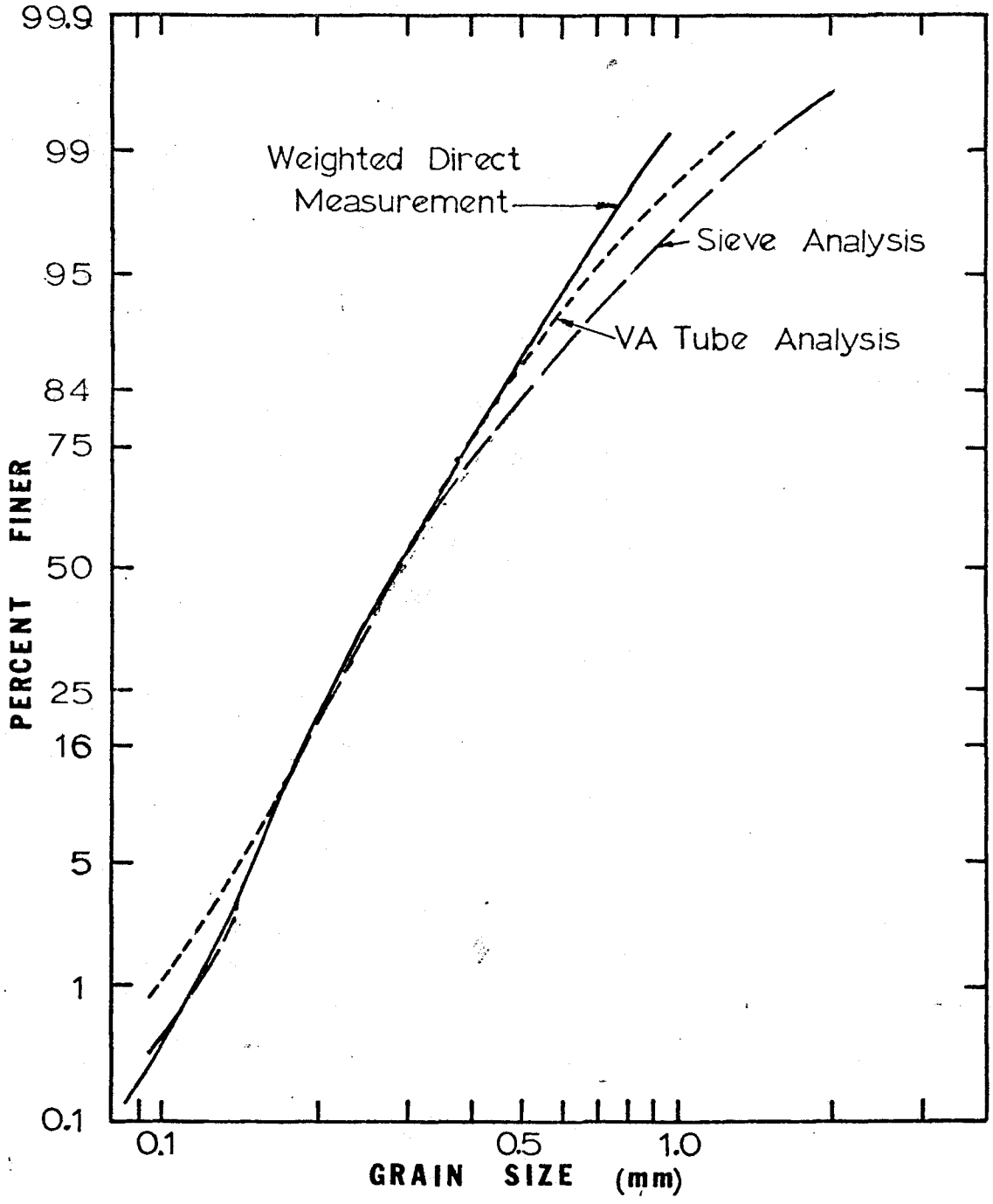

Fig. 11. Size distribution curves of sand used in the flume. Curves plotted from analyses by visual accumulation tube, sieves, and weighted direct measurement are shown.

water had been drained. Median size, as determined by fall diameter using visual accumulation tube (U. S. Inter-Agency Committee on Water Resources, 1958), was .286 mm with a geometric standard deviation (σ) (A.S.C.E. Task Committee, 1962, p. 98) of 1.59, where

$$\sigma = \frac{1}{2}\left(\frac{d_{50}}{d_{16}} + \frac{d_{84}}{d_{50}}\right).$$

A geometric standard deviation, hereafter referred to as gradation, with a value of 1.0 refers to a perfectly size-sorted sand while a value of 3.5 or larger refers to a poorly size-sorted sand. Sieve analysis of the bed material showed a median size of .285 mm and a gradation (σ) of 1.58 while direct measurement of grains with conversion to the weighted sieve size (See Appendix B for a discussion of technique) showed a median size of .287 and a gradation of 1.56.

Weighted median size of the opaque heavy minerals as determined by microscope measurement in the bed material was .144 mm with a gradation (σ) of 1.49.

The total-sediment discharge was determined from samples collected in a width-depth integrated sample collected at the lower end of the flume.[3] Size and gradation of the collected sediment was determined by use of the visual accumulation tube after each sample was dried and split to a workable size.

Size Analysis - Suspended Sediment—Suspended load samples were collected by a siphon with an inside diameter of 0.95 cm. Inlet velocity at the siphon nozzle was adjusted to equal the local fluid velocity by changing the total head on the siphon. Local velocities were determined by a modified Ott

---

[3]The sample is referred to as an integrated sample because it represents a space-averaged value of concentration.

velocity meter. For dune runs 1 and 2, sediment concentration (ppm by weight) profiles were determined at the trough, brink point, and high on the dune stoss side (See figure 6 for dune terminology). Two sediment concentration profiles were measured for the transition run--one in the plane bed reach and one high on the stoss side of one dune. One concentration profile was taken during the plane bed run (table 3). Sediment concentrations were determined at 3.05 cm increments in the vertical profile at each measurement location.

Size analyses of suspended sediment samples were made by use of the visual accumulation tube. Four point samples were analyzed for size from each profile. Three of the samples were taken at locations 3.1, 9.2, and 18.3 cm above the sediment bed. If the depth of flow was less than 33.6 cm at the sample location, the uppermost collected sample (3 cm below the water surface) was used for the fourth sample, otherwise the sample was taken at 33.6 cm above the bed. To determine the mean size of suspended sediment at each vertical profile that is shown in table 2, the point sample median size was weighted by the concentration at each sample point. Appendix D contains the concentration and size analysis for all suspended sediment samples analyzed.

Opaque heavy mineral grains were observed in the suspended sediment samples from each vertical profile location (although not each point sample) in each of the four runs. Table 4 shows the volume percentage of opaque heavy minerals in the suspended load determined by direct measurement (see Appendix B) for each run. Each of the suspended sediment samples from the runs show an opaque heavy mineral content distinctly smaller than that of the bed material samples. Only run 2 had a volume percentage of dark opaque grains approaching that of the bed material.

Table 3.—Concentration and size of total transport load and suspended sediment load.

Run	Bed Form	Total Transport Load			Suspended Load			
		Ave. Mean Conc. (ppm) by wt.	Ave. Size d_{50}* (mm)	Ave. Gradation (σ)	Location	Ave. Mean Conc. (ppm)	Ave. Size d_{50}* (mm)	Ave. Gradation (σ)
1	Dunes	351	.206	1.43	Dune Back	278	.175	1.23
					Brinkpoint**	131	.156	1.28
					Trough	316	.172	1.26
2	Dunes	778	.183	1.47	Dune Back	443	.149	1.30
					Brinkpoint	278	.140	1.32
					Trough	883	.180	1.31
3	Transition	827	.206	1.45	Dune Back	228	.147	1.29
					Flat Bed***	240	.163	1.28
4	Flat Bed	1797	.200	1.59	Flat Bed	1314	.169	1.32

*Size determined by VA tube sedimentation analysis

**Only the lower three sample points used

***Concentration and size are low because the lowest sample was obtained at 7.6 cm above the bed rather than 3.1 cm.

Table 4.--Analysis of opaque heavy mineral grains in suspended sediment.

Run	Total Grain Counts in Samples	Suspended Material Median Size (mm)	Opaque Heavy Mineral Grains		
			Total Grain Counts in Samples	Median Size (mm)	% by Volume
1	2200	.170	8	.103	0.08
2	2600	.165	23	.103	0.22
3	1600	.155	10	.074	0.07
4	800	.169	2	.103	0.06
Bed Material	--	--	--	.144	0.38

By comparison with runs 1 and 4, both runs 2 and 3 had large areas of opaque heavy mineral grains associated with the dune surfaces. Wide areas of opaque heavy mineral accumulations occurred in run 4, but they were generally within the bed or at the base of the sediment flow and not exposed at the surface. In run 1, areas occupied by opaque heavy minerals were small. Although figures 7, 8, and 9 show an increase in turbulence toward the bed and a decrease in turbulence along the length of a dune, no patterns of dark opaque mineral concentrations were observed in the suspended sediments.

Median size of the suspended opaque heavy mineral grains in each run falls below the 20th percentile size determined for the corresponding bed material sample of opaque heavy minerals.

Size Analyses - Core Samples—Opaque heavy minerals and light minerals obtained from the grouted cores were studied to determine whether differences in size and sorting existed among sediments measured in the different runs. Studies of the opaque heavy mineral grains were concentrated on the dark mineral laminations of runs 2, 3, and 4. Only minor accumulations of opaque heavy minerals were present in run 1, and those were insignificant in thickness and areal distribution when compared to those in the accumulations of runs 2, 3, and 4.

Core samples were taken from at least two networks across and along the bed following each flow experiment, at 1.22 meter intervals along the flume and at center line and .61 meter from each wall. Total length of each sample network was selected to include the entire length of at least one bed form present (average length of the networks was 6.1 meters). Samples were taken from small pits into one wall of each of which was inserted a can 6.5 cm in diameter and 12.7 cm in length to obtain horizontal cores. Similar core samples were obtained from large areas of heavy mineral segregation that were missed in the network samples.

Inasmuch as heavy mineral accumulations developed only near the upper surfaces of the sediment, it was necessary that the surface sediments be included in the sample. Therefore, most samples were taken in such a way that a small space above the sediment surface remained at the top of the can. Plaster of Paris was poured into this open area and moisture was allowed to evaporate. A chemical soil grout (AM-9, American Cyanamid Co.) was poured into the sample and allowed to harden. Adhesive strength of the grout was controlled to permit easy removal of sand grains from selected areas. The grouted samples were sawed to remove disturbed portions of the core and the sedimentary structures and segregation of minerals studied in the position that they were deposited.

Selection of cores for analysis was based on the presence and location of concentrated beds of opaque heavy minerals. The method of preparing and a description of grain-mounting grains from a lamina within a core sample is described in Appendix B. Data on grain sizes and gradations for layers of opaque heavy minerals selected from the various core samples are represented in figure 12A (complete analyses of size, shape and gradation are shown in Appendix C, table 8).

In run 2, opaque heavy mineral samples were obtained from topset and foreset beds and from the brink lines of dunes. Samples from run 3 were obtained from topset and foreset beds, and one sample was taken from the flat-bed region. Samples from run 4 were obtained from dark opaque laminae located at the base and within the flat-bedded sands. Measurements of grain size and gradation for samples shown in figure 12A, 12B and Appendix C (table 8) were obtained from direct measurement of 200 individual grains per sample mount.

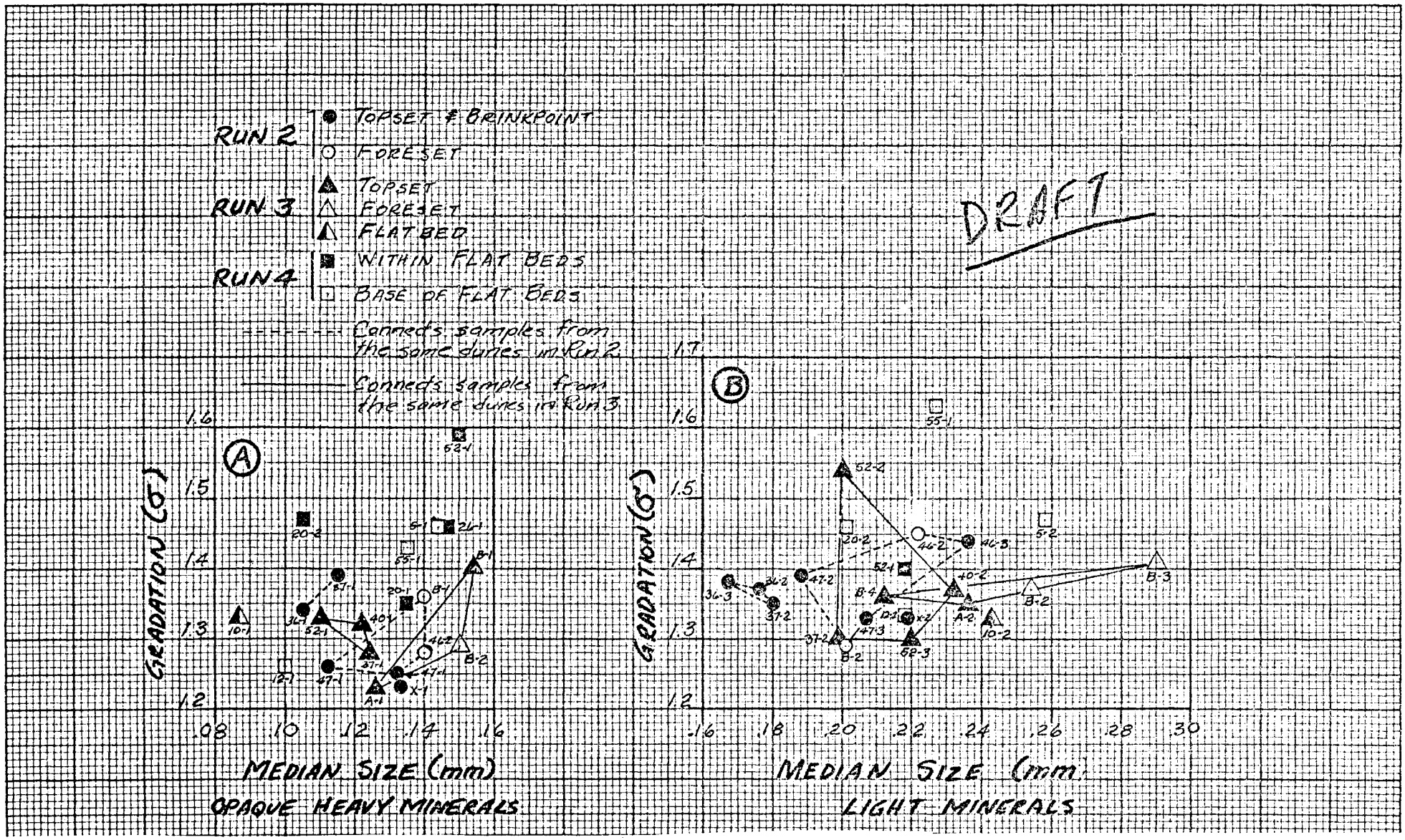

Fig. 12. Median sizes and gradation of grain mounts from core samples obtained from the sediment bed of runs 2, 3, and 4: (A) Opaque heavy mineral samples from heavy mineral laminae, (B) Light mineral samples adjacent to or within the opaque heavy mineral laminae.

Size and gradation analyses made from grain mounts of light minerals were obtained either from light mineral laminae adjacent to or from light minerals present within opaque heavy mineral laminae (fig. 12B).

Analysis of variance tests were conducted for the median size, gradation (σ), and shape factor of opaque heavy mineral grains obtained from core samples from runs 2, 3, and 4. The tests are used to determine whether two or more sample means could have been obtained from populations with the same parametric mean with respect to a given variable, or whether the samples were obtained from different populations (Sokal and Rohlf, 1969, p. 175). In this study the analysis of variance tests were conducted to determine if the sediment properties of the opaque heavy minerals in the segregated layers of each run are significantly different in each run. Since the same sediment was used for each run, any significant differences in the sediment properties between runs must be due to the effect of the different flows on the grains.

Data used for the analysis of variance tests were obtained from laminae of dark opaque minerals in the core samples (Appendix C, table 8), and the results of these analyses are shown in table 5.

The results of the tests on the median grain size and the grain shape factor of opaque heavy mineral grains showed that no differences existed among runs at the 5 percent level of significance. A significant difference, however, did exist in the gradation among runs at the 1 percent level. An a posteriori SNK test (Sokal and Rohlf, 1969, p. 239-246) of the gradation means of the three runs was conducted to determine which run was significantly different from the others. Results of the SNK show that the mean gradation value of the opaque heavy mineral samples in run 4 is significantly different from the other two runs at the 1 percent significance level.

Table 5.---Analysis of variance between runs of median, gradation, and shape factor of opaque heavy mineral samples from runs 2, 3, and 4.

Sample	Source of Variation	d.f.	Sum of Squares	Mean Square	Variance Ratio F	F_{05}	F_{01}
Median	Among Runs	2	.00015	.00008	.205	3.55	6.01
	Within Runs	18	.00694	.00039			
	Total	20	.00709				
Gradation	Among Runs	2	.07326	.03663	6.36**	3.55	6.01
	Within Runs	18	.10366	.00576			
	Total	20	.17692				
Shape Factor	Among Runs	2	.00232	.00116	2.36	3.55	6.01
	Within Runs	18	.00888	.00049			
	Total	20	.01120				

** = (0.01 < Probability < 0.001)

The median size and gradation for light mineral samples that were sampled adjacent to and within the opaque heavy mineral laminae also were tested by analysis of variance tests(gradation and median values of samples are listed in Appendix C, table 9). The tests show that no difference in gradation of light minerals existed between runs 2, 3, and 4; but, a significant difference did exist at the 5 percent level between the median sizes of the samples (table 6). Results of these tests should indicate whether a given flow had an effect on the properties of light mineral grains that were closely associated with opaque heavy mineral grains ~~laminae~~ that differed significantly from the other flows.

A SNK test of the mean of the sample median grain sizes for each of the three runs showed that no significant difference existed between the three runs. However, a SNK test for uneven sample sizes, such as was used for runs 2, 3, and 4, does not provide sufficient sensitivity to determine which run differed significantly from the other two in its effect on sample median size.

between runs

Table 6.--Analysis of variance of median size and gradation of light mineral samples associated with opaque heavy minerals in runs 2, 3, and 4.

Sample	Source of Variation	d.f.	Sum of Squares	Mean Square	Variance Ratio F	F_{05}	F_{01}
Median	Among Runs	2	.00497	.00249	3.89*	3.49	5.85
	Within Runs	20	.01281	.00064			
	Total	22	.01778				
Gradation	Among Runs	2	.03030	.01515	2.67	3.49	5.85
	Within Runs	20	.11368	.00568			
	Total	22	.14398				

* = (0.05 < Probability < 0.01)

EXPERIMENTAL RESULTS

Summary of Bed Form and Opaque Heavy Mineral Sorting Characteristics

Four different flow conditions were observed in this study (table 7); and based on the terminology of Simons and Richardson (1966), two runs were made in the lower flow regime, one run in the upper flow regime, and one run in the transition zone between the upper and lower regimes. A bed configuration consisting of dunes (lower flow regime) existed in runs 1 and 2. Transition bed forms of long profile dunes and a near flat-bed condition existed in run 3, while run 4 consisted entirely of a flat bed formed in the upper flow regime. Average lengths, heights and length/height ratios for the dunes of different runs measured from sonic sounder charts are listed in table 7.

Only thin accumulations of opaque heavy minerals covering small areas were present at the surface of bed forms produced by run 1. All other runs resulted in large accumulations of opaque heavy minerals associated with the bed forms.

Low Shear Dunes (Run 1)--Dunes in run 1 were formed under conditions of much lower shear stress at the bed and a lower Froude number than were the dunes of run 2. In profile the dunes of run 1 were generally triangular in shape with the crest line of the dune coinciding with the dune brink line. Topset beds were only present on a few dunes in run 1. The average angle of inclination of the foreset beds in run 1 was 32.4° with a standard deviation of 2.3°. Configuration of the dunes forming the bed surface (fig. 13A) can best be described as linguoid. Rates of movement of the dunes ranged from 0.6 to 1.0 meter per hour.

Accumulations of opaque heavy minerals associated with the dunes were limited to small, very thin ripple-form accumulations on the stoss slopes of the dunes (fig. 13B). The small thin accumulations of opaque heavy minerals appear to develop just downstream of the reattachment point (the

Table 7. - Mean dune size (with standard deviation).

Run	Number of Dunes Measured	Height* (cm)	Length** (m)	L/H Ratio
1	115	10.2 ± 4.9	1.63 ± 0.66	18.2 ± 8.7
2	28	30.0 ± 13.2	7.24 ± 4.67	26.3 ± 15.0
3	46	12.3 ± 6.8	5.66 ± 2.48	46.6 ± 29.6

*Dune height determined by maximum vertical distance between the trough point and the summit point of the dune as measured on the sonic sounder profile.

**Dune length was determined from the low trough point between dunes to the next trough point downstream as measered on the sonic sounder profile taken along the centerline of the flume.

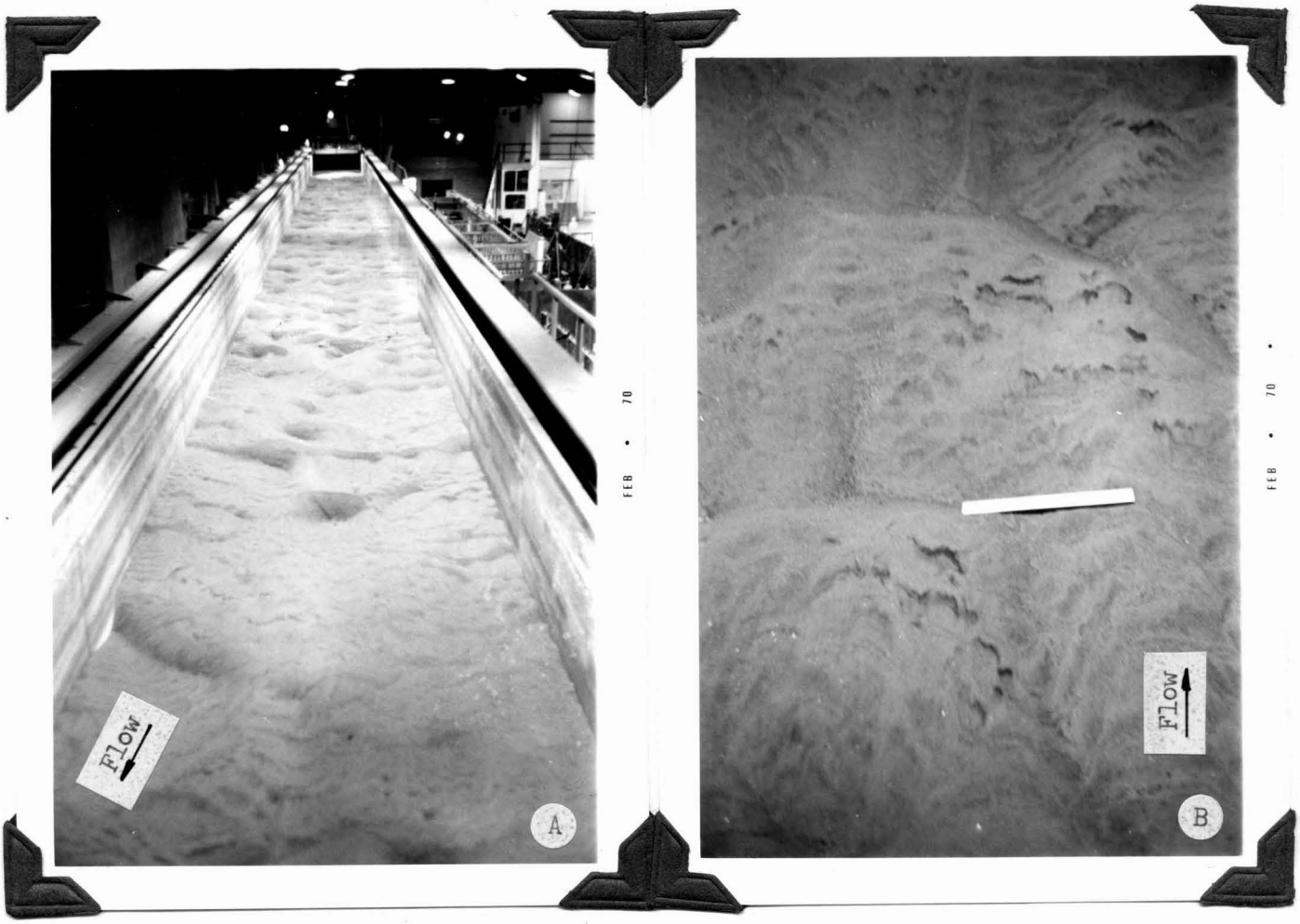

Fig. 13. Dune bed configuration and opaque heavy mineral accumulations at the bed surface following run 1. (A) Dune-bed configuration (view upstream), (B) Stoss slopes of dunes showing small areas of concentrated opaque heavy minerals (length of rule - 30.5 cm).

location where the flow impedes on the back of the downstream dune after it has passed over the upstream dune front) and migrate up the dune stoss slope. No accumulations of opaque heavy minerals were observed in the foreset beds.

High Shear Dunes (Run 2)--Dunes formed by flow conditions in run 2 (table 2) were longer and higher than dunes produced by other runs. Distances between brink lines and crest lines of dunes commonly ranged from 25 to 110 cm, and averaged 60 cm. Topset beds were present on most dunes with the total thickness of topsets ranging up to 3 cm. Foreset beds of the deposits in run 2 showed an average dip of 29.2° and a standard deviation of 3.1°. Generally the inclination angles of the foreset beds ranged from 28° to 32° but some low bed angles of 21° to 23° existed that indicate unstable conditions in the dune development. Dune fronts in run 2 were sinuous across the width of the flume (fig. 14, 15), and rates of movement of the dunes down the flume (based on successive brink line locations) ranged from 1.5 to 3.4 meters per hour.

Accumulations of opaque heavy minerals were associated with the dunes (fig. 16) and commonly were present as:

1. Accumulations of opaque heavy minerals on the dune stoss slopes that formed thin ripple-form accumulations and very thin, almost sheet-like accumulations. The thin ripple accumulations resembled those shown in figure 13B and were very common on the dune stoss slopes. The ripple accumulations appeared to have originated on the lower part of the dune stoss slope and migrated up the dune. Thin sheet-like accumulations of the opaque heavy minerals such as shown in figure 15 were present on many dune stoss slopes.

2. Thick accumulations of opaque heavy minerals that formed on the high portions of the dune associated with the dune crest area. These accumulations formed the thickest beds of opaque heavy mineral accumulations

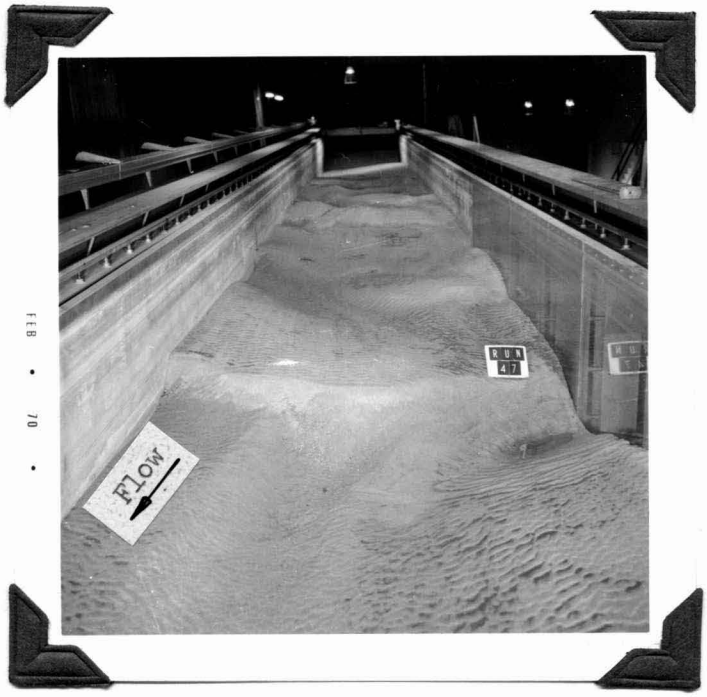

Fig. 14. Dune-bed configuration (view upstream) of run 2. Figure 15 is a close view of the large dune in the center of the photo on which the sign is located. The sign on the photo and other photos of dune runs indicates the run number of the U.S.G.S. continuing series of different flow conditions using the same bed-material size.

Fig. 15. Accumulations of dark opaque heavy minerals on the upstream sides of dunes (run 2). Location of cut-away view of dune (fig. 17) is shown by the line near the flume wall on left side of photo. The ripple surface that is shown on the dune is due to abrupt changes in hydraulic flow conditions that occurred when the flume was shut down at the end of the run.

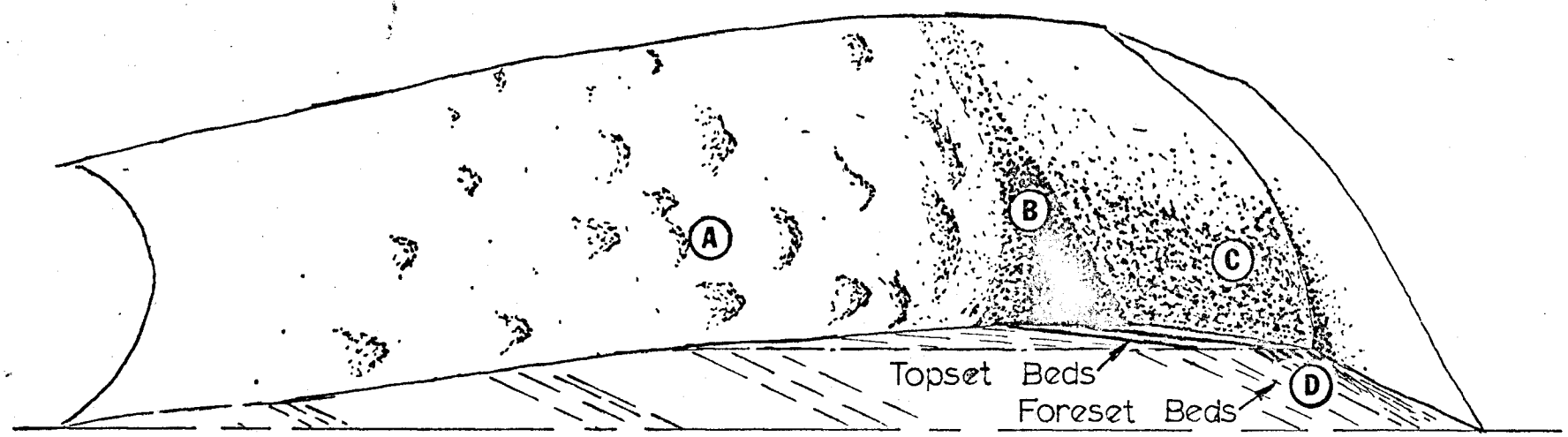

Fig. 16. Generalized dune cut-away showing structure and location of different types of opaque heavy mineral accumulations: (A) Thin ripple accumulations on stoss slopes, (B) Crestal region accumulation, (C) Region between the crest line and brink line where accumulations occur, and (D) Accumulation in foreset beds. (3x vertical exaggeration)

observed and the beds were nearly 100 percent efficient in opaque heavy mineral segregation. Observations made through the plexiglass wall of the flume during the flow showed that the opaque heavy mineral accumulations formed on the highest portion of the dune (in dune profile). The accumulation as a whole moved downstream at a rate approximately equal to the rate of movement of the dune. Scour occurred periodically both upstream and downstream in areas adjacent to the heavy mineral area. When degradation immediately downstream of the heavy mineral area reached approximately 1 to 2 cm below the high point of the accumulation, a large amount of the heavy minerals was transported from the accumulation by suspended and tractive movement.

3. Accumulations of opaque heavy minerals that were deposited between the dune crest line and the brink line. These deposits, derived from the thick crest area concentration of opaque heavy minerals, form part of the topset beds of the dune. An example of numerous opaque heavy mineral laminae in the topset beds is shown in figure 17B.

4. Accumulations of opaque heavy minerals at the brink point and deposited on the slip face of the dune. These deposits formed dark laminae in the foreset beds like those shown in figure 17A. The concentrated opaque heavy mineral layers did not extend down the foreset beds more than 8 cm (total slip face length on the dunes commonly was between 20 and 30 cm) and a decrease in concentration of heavy minerals occurred with increased distance down the concentrated bed from the brink line. Losses of opaque heavy minerals from the topset beds occurred by tractive and suspended transport over the brink point.

Transition Bed Forms (Run 3)--The flow of run 3 had a higher Froude number than the two dune runs but a lower Froude number than the flat-bed flow.

During the run the bed forms alternated between large dunes (fig. 18A, 18B) and a near flat-bed condition (very long profile dune). The near

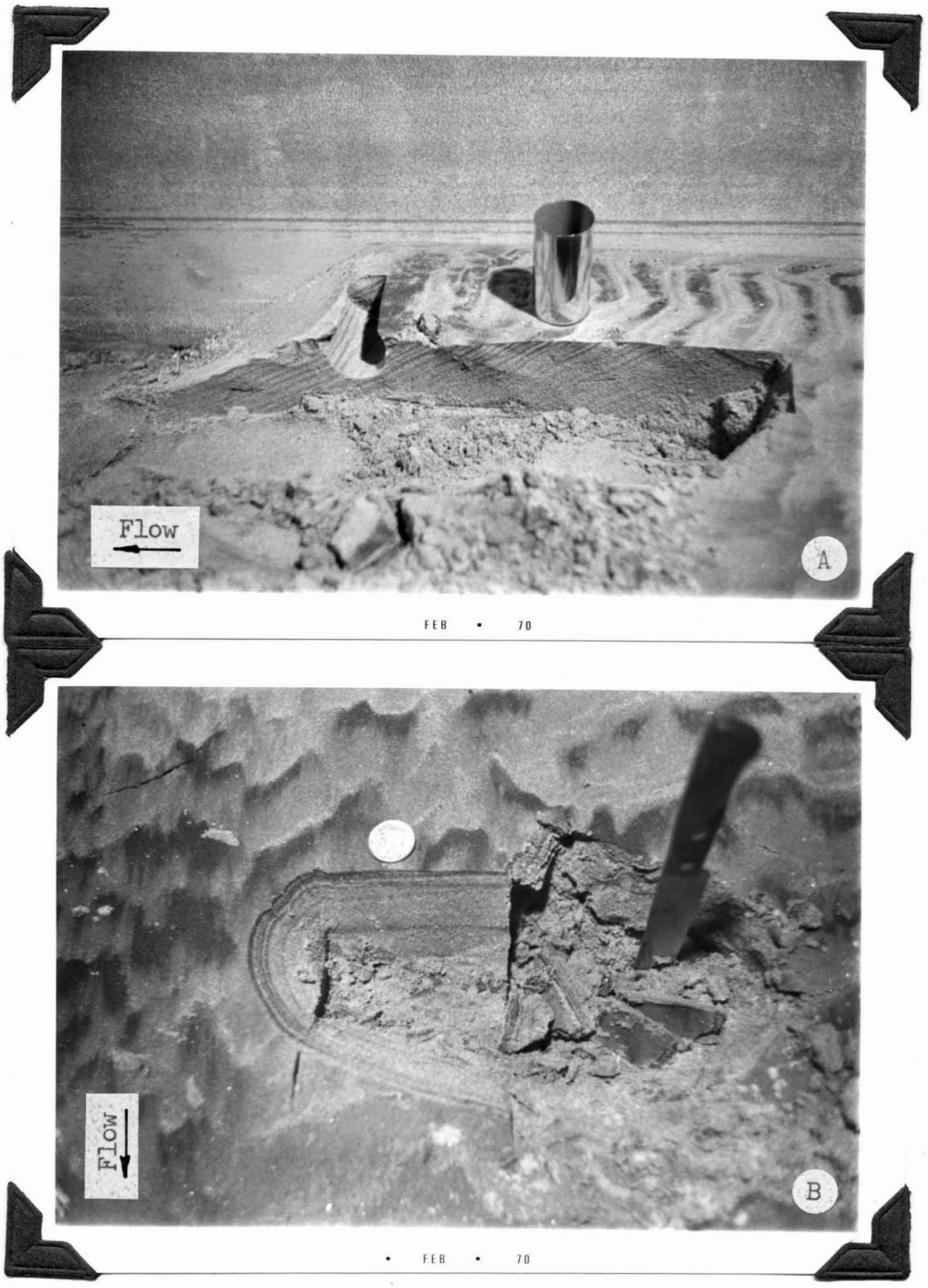

Fig. 17. Opaque heavy mineral accumulations in foreset and topset beds of dunes formed in run 2. (A) Cut-away portion (60 cm long) of dune in figure 15 showing concentration of opaque heavy minerals (dark beds) in the foreset beds, (B) Segregation of opaque heavy mineral grains in topset laminations.

Fig. 18. Bed configuration and opaque heavy mineral accumulation at the bed surface formed during run 3. (A) Dune region of transition flow (view upstream), (B) Close-up view of dunes showing opaque heavy mineral segregation on the dune stoss slopes. Signs in photos refer to number of the flow in continuing experiments of U. S. Geological Survey. Ripples present on the dunes were not present during the run but were formed as the result of abrupt changes in flow conditions during flume shut down.

flat-bed condition of the run differed from a true flat bed because at no time did the flat bed extend the entire length of the flume. In addition, the near flat-bed condition differed from the flat bed of run 4 by having a slip face on its downstream edge as well as slight form irregularities on its surface. Dunes associated with run 3 had a much larger L/H ratio than the dunes of runs 1 and 2.

Dunes of run 3 had a distance from the crest line to the brink line that was commonly 15 to 85 cm with a mean distance of 53 cm. In some cases the distance was as large as 2.5 meters. Topset beds were present on virtually all the dunes. Dune fronts were sinuous across the flume as shown in figures 18A and 18B. Angles of inclination of foreset beds averaged 28.6° with a standard deviation of 3.2°. Several foreset dip values of 21° to 23° indicated local conditions of unstable deposition. Rates of movement of the dune fronts ranged from 2.7 to 4 meters per hour.

Opaque heavy mineral accumulations were common in association with the transition bed forms. Accumulations were located in the near flat bed and at various locations on the dunes. In summary, the opaque heavy mineral segregations were present as:

1. Thin but widespread accumulations near the bases of flat beds, just above foresets formed with or as part of dunes deposited earlier.

2. Layers of concentrated opaque heavy minerals within laminations in flat beds. These opaque heavy mineral layers were usually thinner than the opaque heavy mineral beds at the base of the flat-bedded sediments.

3. Accumulations associated with the dune phase of the transition bed forms. They were basically the same as the opaque heavy mineral accumulations associated with the dunes of run 2, namely:

a. Thin ~~concentrations~~ accumulations of opaque heavy minerals in ripple-form and sheet-like ~~concentrations~~ accumulations that advance up the stoss side of dunes.

b. Thick opaque heavy mineral ~~concentrations~~ accumulations that were commonly present along the crestal region of the dune (fig. 19A, 19B).

c. ~~Concentrations~~ Accumulations that were present downstream from the crest line and extending to the brink line (fig. 20A, 20B). In several dunes the opaque heavy mineral segregation was observed in the foreset beds as shown in figure 20A.

d. Thick ~~concentrations~~ accumulations were often present in the topset beds. These deposits resulted from burial of surface ~~concentrations~~ accumulations of opaque heavy minerals.

Bed Forms of Moving Flat-Bed Conditions (Run 4)--The flow that produced the flat beds of run 4 had the highest shear stress and Froude number of any of the four runs. Under equilibrium flow the sediment bed had an essentially featureless surface (fig. 21). Bed elevation at any point departed only a few centimeters from the mean elevation. A study of bed surface elevation fluctuations at one location during the equilibrium flow showed a maximum fluctuation of only 1.8 cm in a 12 hour period. Studies by Guy, Simons, and Richardson (1966, p. 24, 29) show vertical fluctuations of flat-bed surfaces during several runs as ranging from 1 to 3 cm. Bedding structures were all flat lying and covered pre-existing bed forms. Total thickness of the flat beds in the run was usually less than 3 cm.

Of the four runs studied in detail, total sediment concentrations in the total-load and suspended-load samples were by far the largest in run 4.

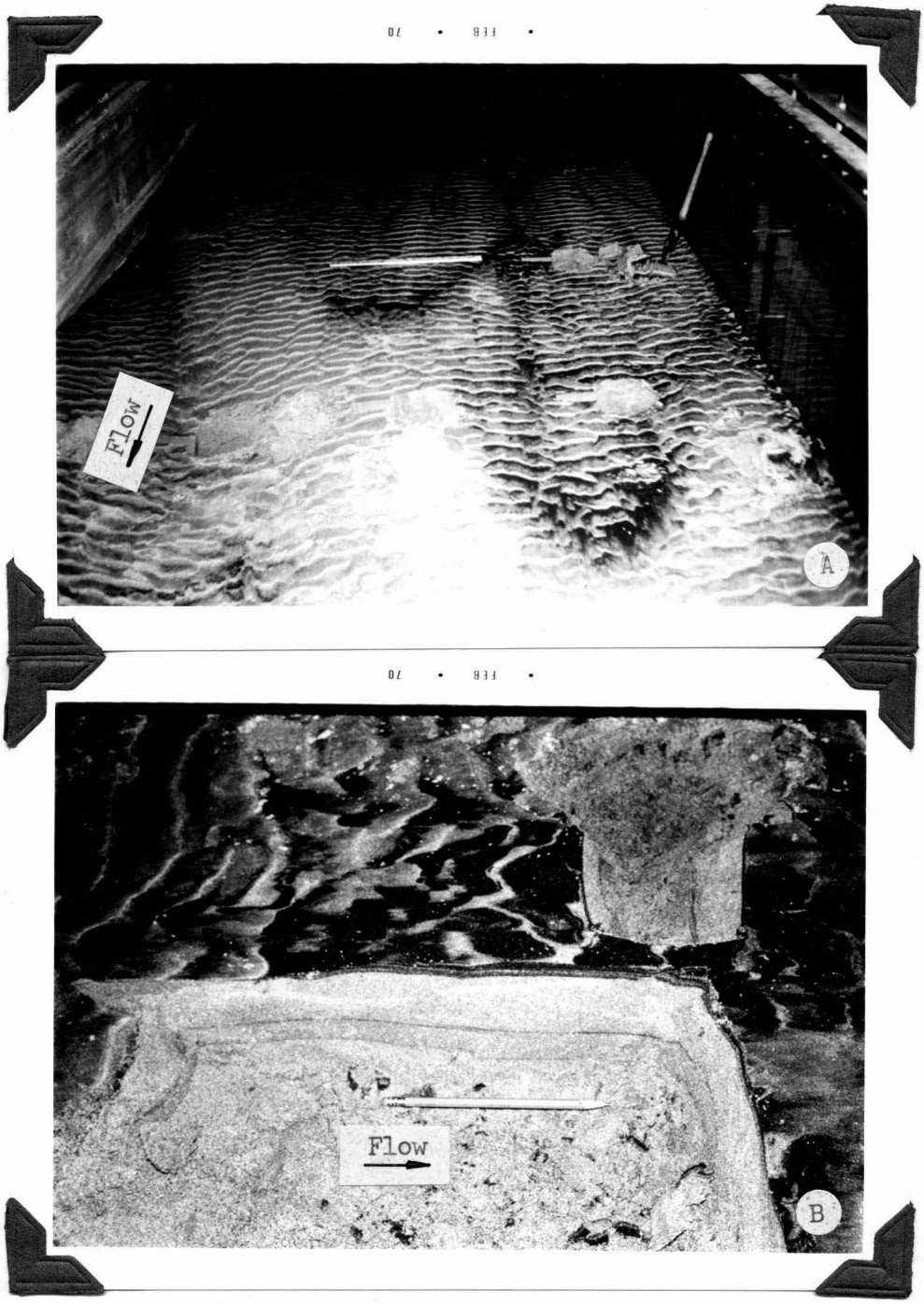

Fig. 19. Accumulations of opaque heavy minerals formed along the crestal region of a dune (run 3). (A) Opaque heavy mineral accumulation on the crestal region of a long dune in the transition flow (view upstream), (B) Exposed topset beds (located at the right side of the 71 cm rule, fig. A) showing the thick dark opaque heavy mineral accumulation.

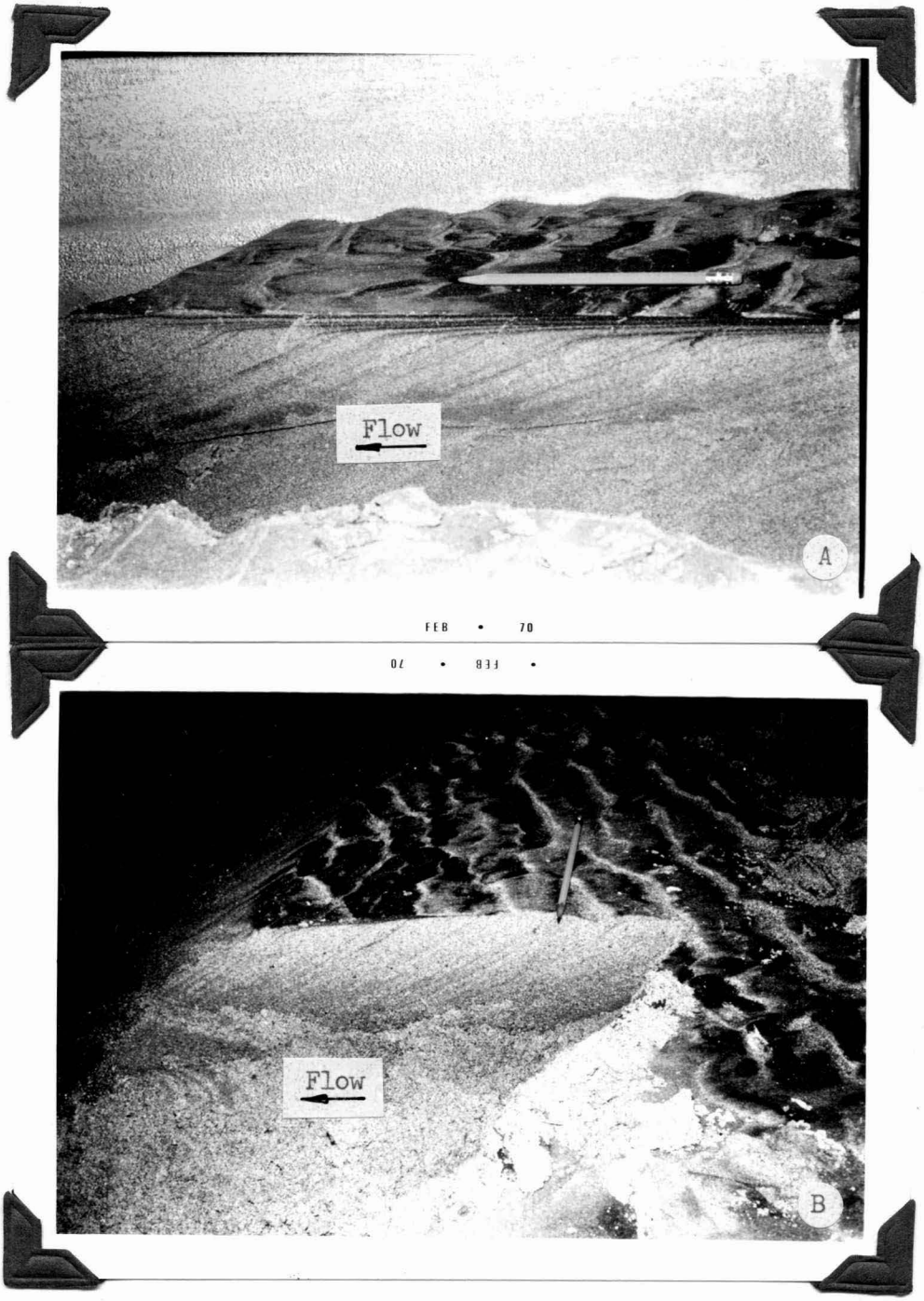

Fig. 20. Opaque heavy mineral accumulations formed in topset and foreset beds during run 3. (A) Opaque heavy minerals (dark laminae) in topset beds near the brink line and in the foreset beds after passing over the brink point, (B) Foreset beds with very few opaque heavy minerals present, but a large amount of opaque heavy minerals are present in the thin topset beds.

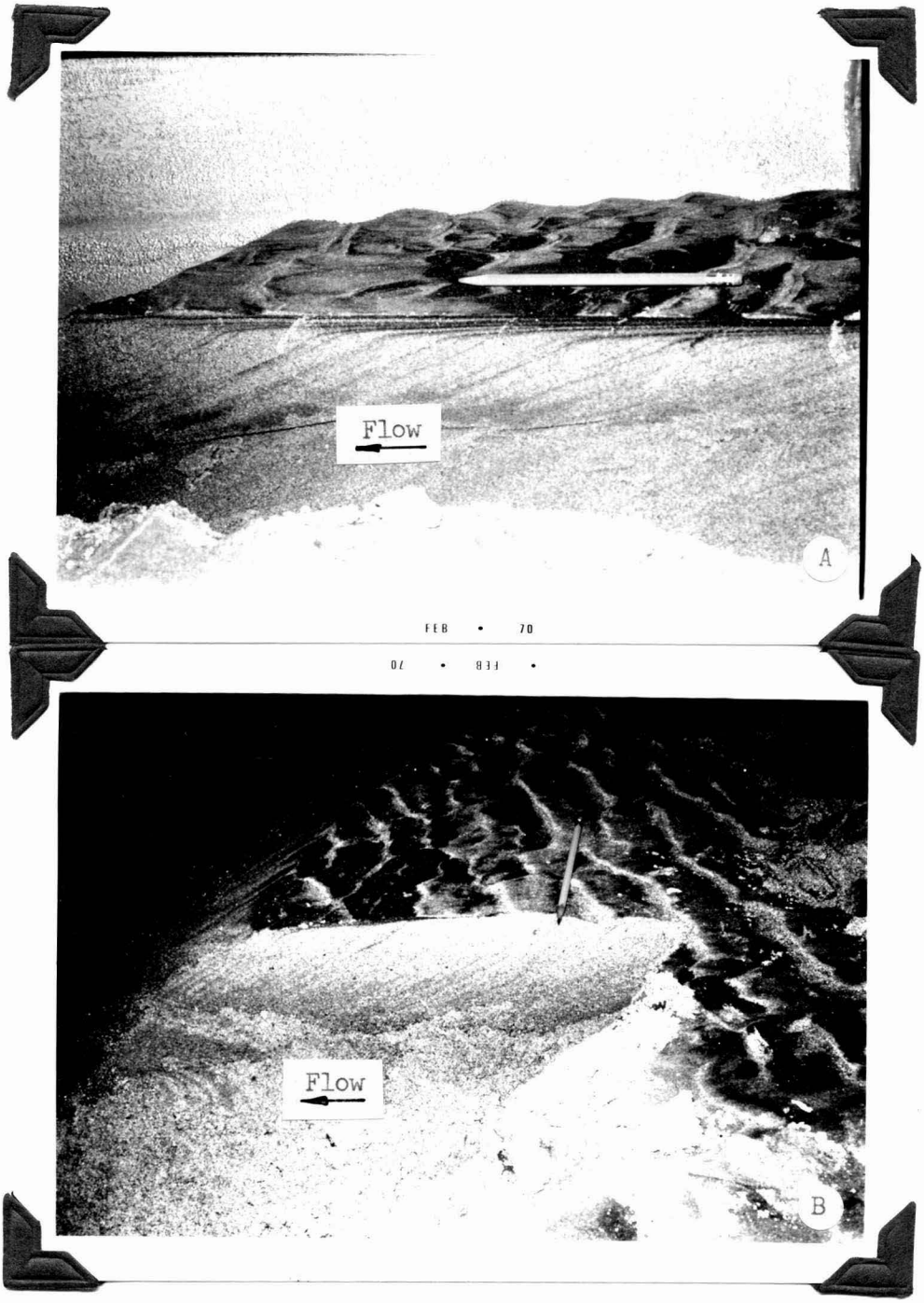

Fig. 20. Opaque heavy mineral accumulations formed in topset and foreset beds during run 3. (A) Opaque heavy minerals (dark laminae) in topset beds near the brink line and in the foreset beds after passing over the brink point, (B) Foreset beds with very few opaque heavy minerals present, but a large amount of opaque heavy minerals are present in the thin topset beds.

Opaque heavy mineral accumulations were common in the flat-bed runs and accumulations of the heavy minerals were present at the base of and within the flat beds over virtually the entire flume area. The individual beds, however, tended to lense out within a few meters. Accumulations were often the thickest and most widespread at or near the bases of the flat beds. Dark opaque mineral accumulations in the flat beds (fig. 22) usually were not as thick as the heavy mineral laminae at the base of the flat beds. In run 4 no opaque heavy mineral accumulations were present at bed surface.

Relation of Fall Velocities of Dark Opaque and Light Density Grains

Samples of light minerals obtained from laminae adjacent to or located within laminae having a high concentration of opaque heavy minerals were studied to examine relations of fall velocities of associated light and heavy mineral grains.

In order to compare fall velocities, a graph relating sieve size to fall velocity for grains with a 0.7 shape factor and specific gravities of 2.65 and 5.0 was plotted (fig. 23) from data reported by the U. S. Inter-Agency Committee on Water Resources (1957). Values of fall velocities for the d_{16}, d_{50}, and d_{84} grain sizes were determined from figure 23 using the samples described in Appendix C, tables 8 and 9. These fall velocity values are listed in Appendix E. Fall velocity relations between opaque heavy mineral grains and light mineral grains of the bed material sample and the average of all the core samples are shown in figure 23. Using the range between the 16th and 84th percentiles of the opaque heavy mineral grains and the light mineral grains for the sampled laminae in the core samples, the average for the core samples shows 78 percent of the light mineral grains having fall velocities within the same range as 80 percent of the opaque heavy mineral grains. For the bed material samples,

Fig. 21 Flat-bed surface (view upstream) formed by run 4. The sign represents continuous series number. Ripples at the surface were due to shut down of the flume.

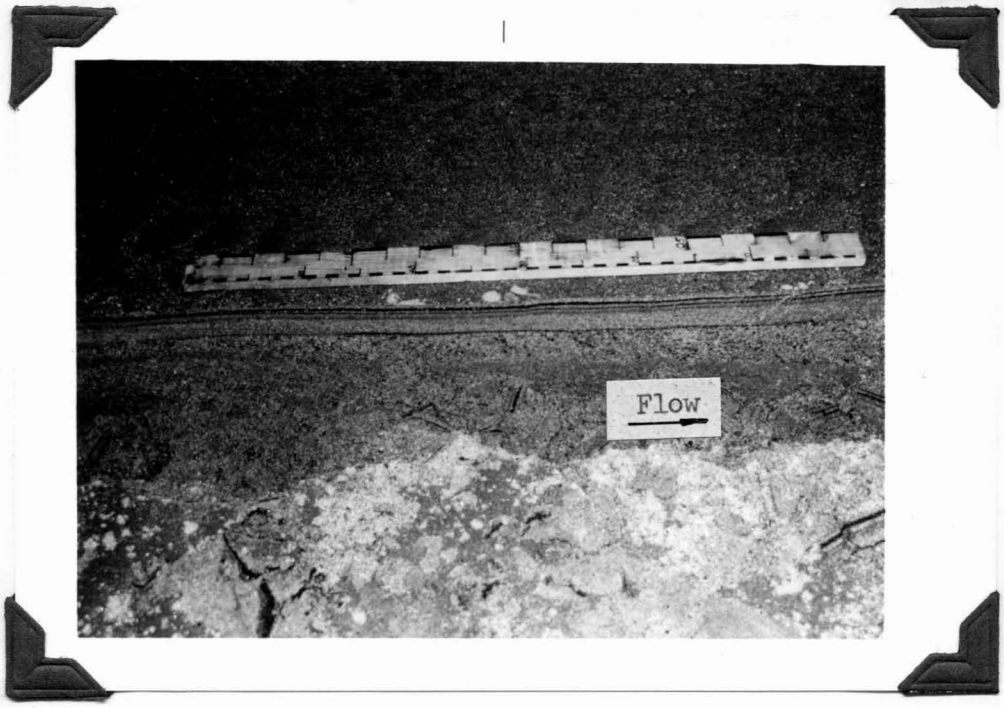

Fig. 22. Profile of flat-bed structure showing segregation of opaque heavy minerals (dark beds) in the flat-lying beds. The lower dark mineral bed is directly overlying foreset beds of an earlier run. Wavy appearance of the dark laminae in the photo is due to an irregular cross-section cut. Small areas of dark mineral laminae in the foreground are fragments of bed material cut away from the cross-section cut and are not part of the bed. The rule is 71 cm in length.

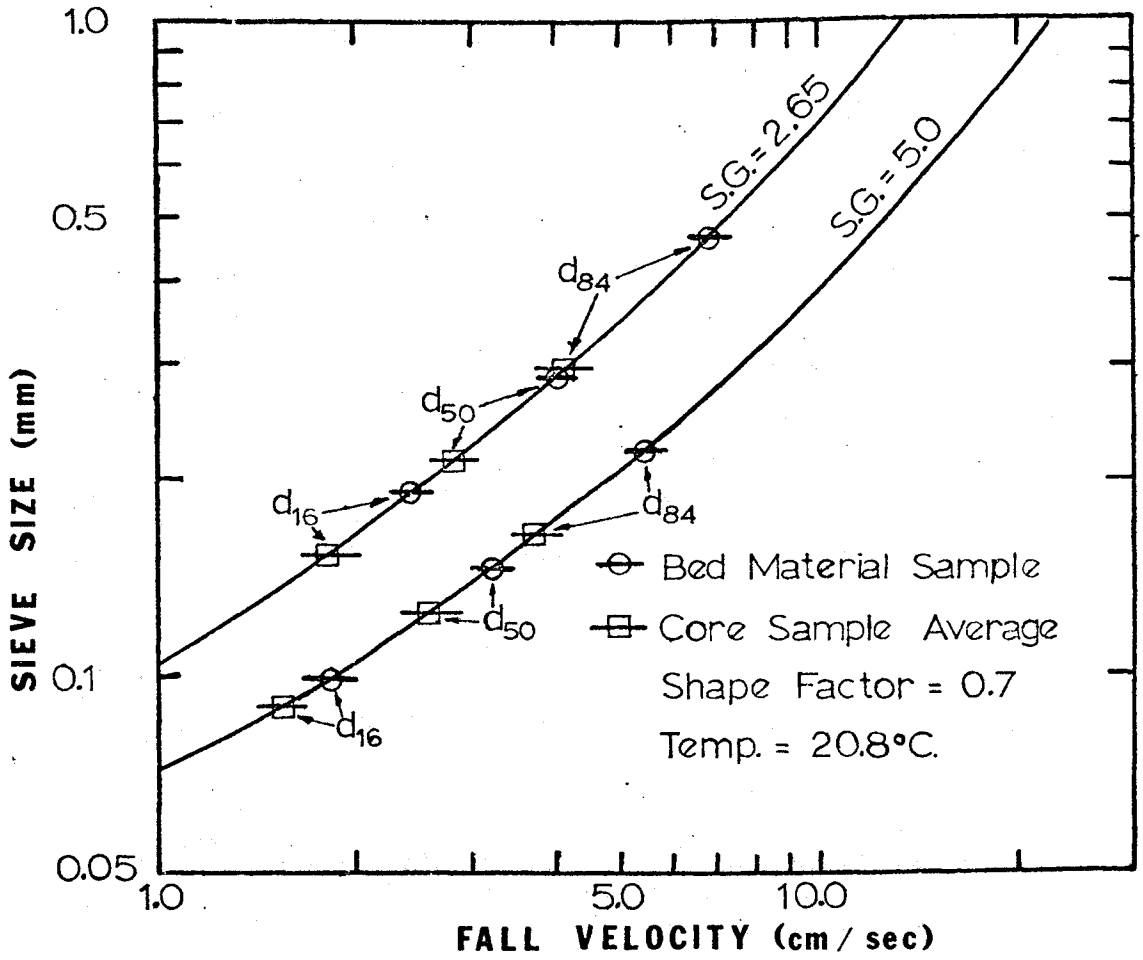

Fig. 23. Fall velocity relationship of light mineral grains to opaque heavy mineral grains obtained from the bed material sample and core samples of runs 2, 3, and 4.

74 percent of the light mineral grains had fall velocities equivalent to 78 percent of the opaque heavy mineral grains.

Median fall velocity values of the opaque heavy minerals and the median fall velocities of light minerals sampled adjacent to (18 samples) or within (5 samples) the opaque heavy mineral laminae have a correlation coefficient of .369 (fig. 24) a value that suggests that no correlation exists. The lack of correlation for medians of fall velocity between the two mineral groups shows that the median fall velocity of one group is not a predictor of the median fall velocity of the other group. With large ranges of grains having equivalent fall velocities existing for the two mineral groups in adjacent laminae, the lack of correlation for mean fall velocities of the opaque heavy minerals and light minerals suggests that other factors were much more important for the occurrence of local sorting.

Relation of Grain Entrainment to Critical Shear Stress and Grain Size

Based on the Shields diagram (fig. 4) one can develop the relation of critical shear (τ_c) to grain sizes for grains of different densities.

Such a series of curves was developed by Grigg and Rathbun (1969, p. 79). Two curves similar to Grigg and Rathbun's are plotted in figure 25 for grains of 5.0 and 2.65 specific gravities. The range between the 16th and 84th percentiles of the opaque heavy mineral grains and the light mineral grains of the bed material and the average values for the sampled laminae in the core samples from runs 2, 3, 4 are plotted in figure 25 to show that a large difference exists in critical shear between the two mineral groups. This difference in critical shear indicates that movement of the quartz and feldspar grains from sands in this study would occur much more readily than the magnetite and ilmenite grains.

Distinct differences in physical size between grains of two different densities but equivalent fall velocities lead to a "hiding effect,"

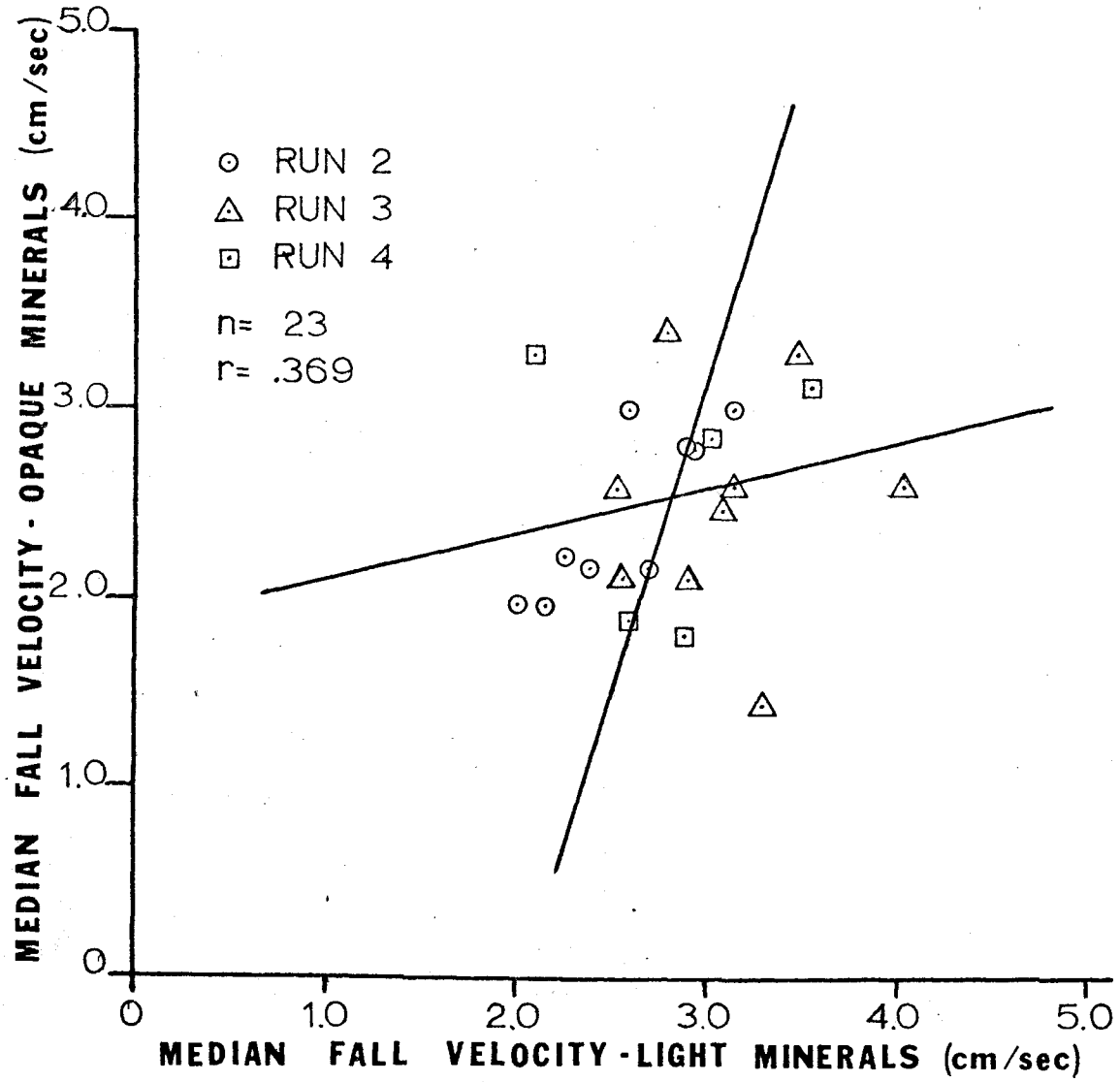

Fig. 24. Plot of median fall velocity of opaque heavy mineral grains and light mineral grains from samples listed in table 11 of Appendix E.

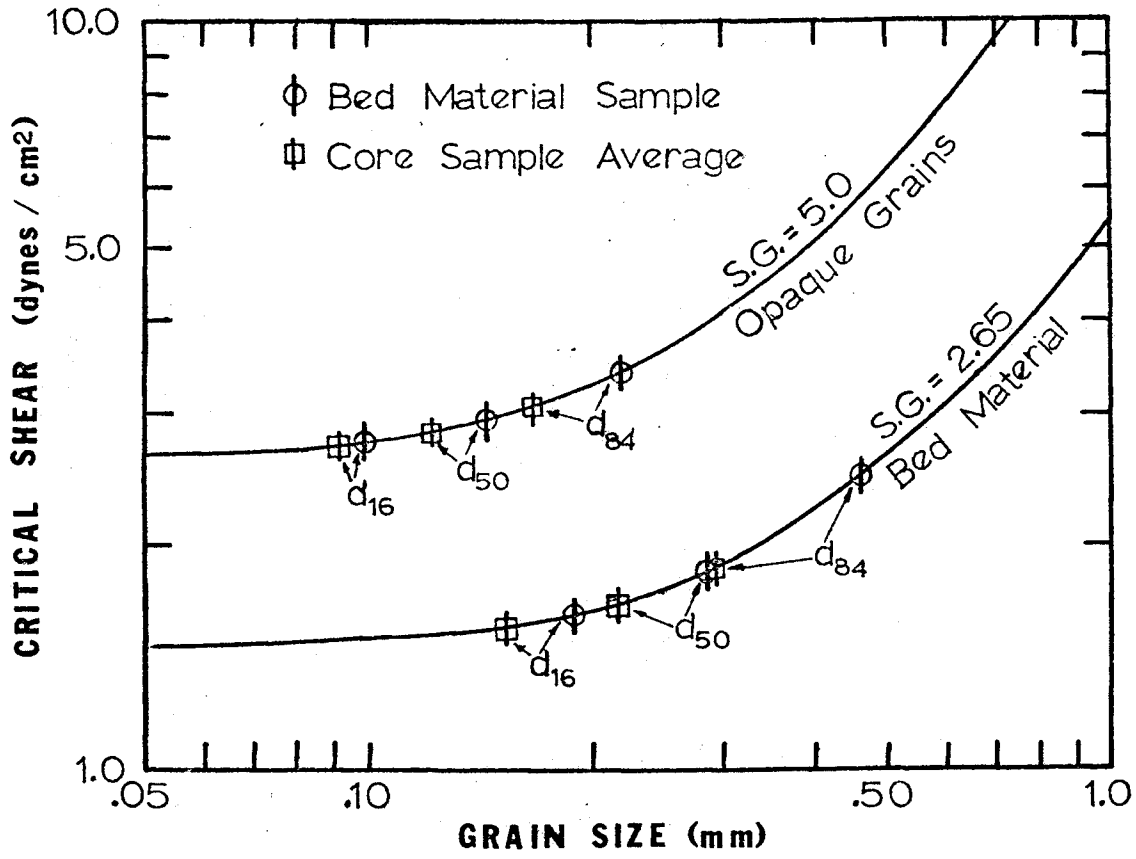

Fig. 25. Critical shear relationship of light minerals to opaque heavy minerals for bed material and core samples.

or a shielding of the smaller grains by the larger grains from flow parallel to the bed. In the size ranges of samples in this study, dark opaque grains and light density grains with equivalent settling velocities have a physical diameter ratio of approximately .58 to .62. The larger, less dense grains would be selectively removed before the smaller grains due to physical exposure to flow alone. When the small dense grains form a small part of the surface bed material such as the dark opaques in this study prior to segregation, a "hiding effect" becomes a significant factor.

Heavy Mineral Transport and Deposition in a Flat-Bed Flow

Observations of bedding structures produced by the flat-bed run (run 4) showed a widespread distribution of dark opaque mineral accumulations. These accumulations of opaque heavy minerals, especially with a thick accumulation occurring at the base of the flat-bedded sands, suggested that the heavy minerals may have concentrated at the base of the tractive load during degradation and were the first deposited during aggradation.

To test the hypothesis of heavy minerals forming as lag deposits during a flat-bed flow, a study was made of the transport of heavy minerals relative to time under equilibrium hydraulic conditions. A small recirculating water-sediment flume (10 cm deep, 20 cm wide, and 10 m long) was used in the experiment with a sand bed of the same Rio Grande sand that was used in the large flume runs. The sand bed was thoroughly mixed after the flow was started. Mixing of the sand provided maximum possible exposure of heavy minerals to the flow. The recorded duration of the run was started just after the mixing of the sand.

A flat-bed condition was established and maintained throughout the study. Hydraulic conditions necessary to form the flat bed were held as constant as possible throughout the run which continued for 47 hours.

Average discharge for the run was 10.98 liters/sec with an average water depth of 7.36 cm. Water surface slope was .0045, and the average temperature was 16.9° C. Total load samples containing 80 to 135 grams of sediment were collected at close time intervals (15 minutes) early in the study with increasingly longer time intervals (up to 7 hours) as the study progressed. Total load concentrations for the study averaged 2699 ppm.

Sediment from the total load sample that passed the 60 mesh (.25 mm) sieve was retained for magnetite separation. Magnetite less than .25 mm was used in this study as the marker mineral because of ease of separation of magnetite and the size was chosen because 88 percent of the dark opaque minerals of the bed material sample were finer than .25 mm. A strong hand magnet was used to separate the magnetite grains from the sample and the percentage of magnetite relative to the total sand passing the 60 mesh sieve was calculated. Results of these percentage plots relative to time (fig. 26) confirm the hypothesis that in a flat-bed flow under equilibrium conditions there is decreasing volume of transport of heavy minerals with increased time.

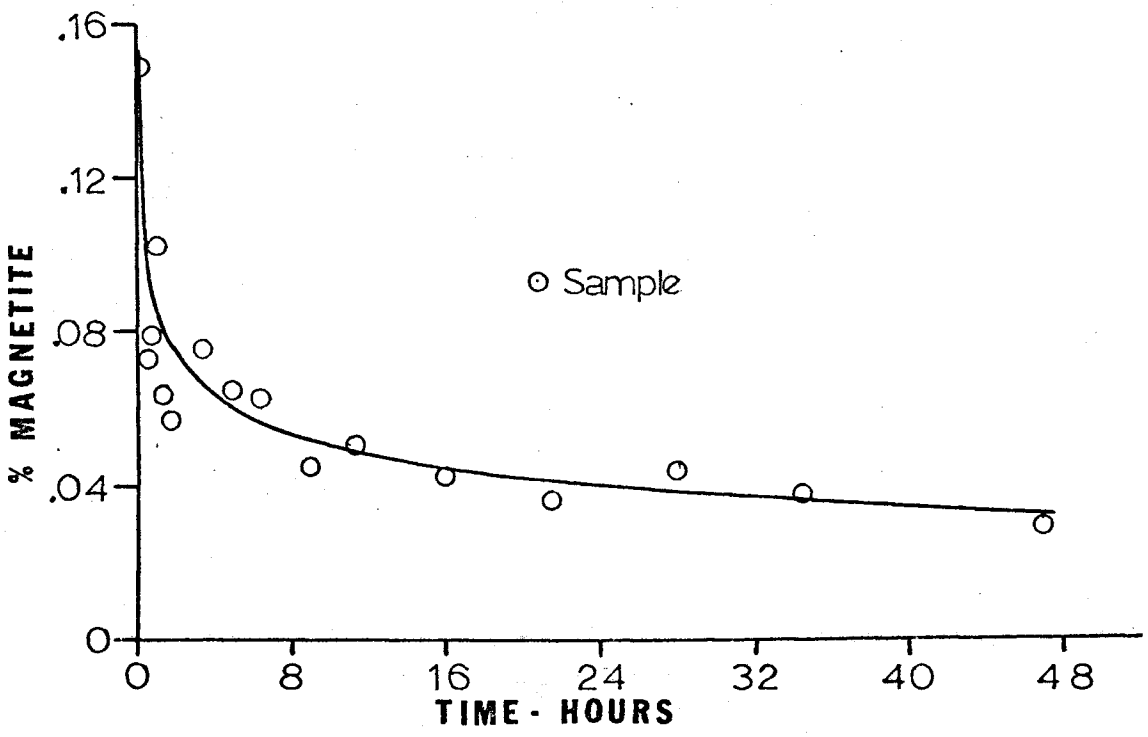

Fig. 26. Relation of magnetite in transport to time in 20 cm flume—flat-bed conditions.

DISCUSSION OF DATA

Relations among Sediment Samples

Light mineral grains and opaque heavy mineral grains in adjacent laminae had large ranges of ~~equivalent~~ equal fall velocities. However, comparison of fall velocities of median sizes of the dark opaque mineral samples and light mineral samples from the core samples showed that no correlation exists (correlation coefficient of .369) for the median values of these two groups. The light mineral samples were obtained from within (5 samples) and adjacent to (18 samples) the opaque heavy mineral laminae. All the light mineral samples were within 2 mm of the heavy mineral laminae. This lack of correlation even when an adequate supply of both mineral groups having equivalent fall velocities were available suggests that factors other than grain fall velocity were much more important to the occurrence local sorting.

Gross transfer of the sediment load, however, may be related to the settling velocities. This relation is suggested by the bed-material samples in which the fall velocities of 78 percent of the opaque heavy mineral grains overlap those of 74 percent of the light mineral grains in the size distribution range between the 16 and 84 percentiles.

Suspended sediment grain analyses indicated that transport of opaque heavy minerals in suspension does not contribute to the opaque heavy mineral segregation. This was indicated by a very low heavy mineral concentration in the suspended sediment even though dark opaque mineral accumulations were located at or near the surface. In none of the runs was there higher percentage by volume of opaque heavy minerals in the suspended sediments than was present in the bed material sample. Total opaque heavy minerals in the suspended sediment samples of the runs were less than 0.3 percent.

Relative Size of the opaque heavy mineral grains in the suspended samples and those in the bed material also precludes the idea of suspension of heavy minerals being the sorting mechanism. All but two of the opaque heavy mineral samples obtained from the bed cores had larger median sizes than the median size of opaque heavy mineral grains from the suspended sediment samples. Intense turbulent conditions of the flow, however, may temporarily suspend ~~light~~ low density ~~material~~ grains allowing a better segregation of the ~~heavy~~ high density ~~material~~ grains.

Analysis of variance tests of median sizes and shape factors of opaque heavy mineral grains obtained from laminae having high concentrations of opaque heavy minerals show that no significant variance at the 5 percent level existed between runs 2, 3, and 4. There was, however, a significant difference at the 1 percent level in the gradation coefficient between the three runs. Among the light minerals from runs 2, 3, and 4 sampled from laminae adjacent to the opaque mineral laminae, a significant difference existed in the median size at the 5 percent level, and no significant difference (5 percent level) existed for the gradation values.

Much larger gradation coefficients existed for opaque heavy mineral samples from run 4 than the other runs. Gradation coefficients for opaque heavy mineral samples of run 4 were close to those of dark opaque grains in the bed material samples. This indicates that all sizes of the high density material in run 4 were being moved by the flow, while sorting of opaque heavy minerals towards finer sizes was occurring in runs 2 and 3.

Sorting, as indicated by the gradation ~~factor~~ coefficient, is the most likely grain distribution parameter affected by the different hydraulic conditions. In the flat-bed flow (run 4) segregation apparently occurred at the base of the bed load forming a widespread layer of opaque heavy mineral grains. As local erosion of the bed occurred, the opaque minerals became concentrated and subsequent deposition allowed preservation of the dark laminae.

For such a concentrating mechanism, the gradation would have a wide range of values and would depend on the ability of the local flow to sort the sample as to size. In the dune flows, sorting as to size was more effective as is shown by their lower gradation values.

Analysis of the critical shear conditions for grain movement indicates that the larger low density grains of the bed material require a much smaller shear for movement than the smaller, more dense grains. Relations of velocities of heavy minerals and light density minerals (fig. 2, 3) and the critical shear relationship of opaque heavy minerals to the bed material sample (fig. 25) all seam to support the idea that the less dense grains are much more readily entrained and moved. In addition, a difference in size between the low density grains and the high density grains leads to a "hiding effect" that can effectively shield the smaller grains from the flow.

Turbulence is more intense in the trough region than on the higher portions of the stoss side or near the brink point of the dune; and, in general, turbulence is more intense near the bed. A large shear stress at the bed caused by the turbulent eddies is probably an important factor in the movement of the opaque heavy minerals, especially in the region of the re-attachment point.

Intermittency of turbulence was not studied quantitatively, but the presence of strong turbulent eddies passing over the crestal region was observed in the flow and its presence is suggested by the laminae of opaque heavy minerals in the topset beds. Strong turbulence to increase local shear could cause a rapid movement of the opaque heavy mineral grains from the ~~summit~~ crest line toward the brink line--and the low density material could then move rapidly over the dense grains or be carried temporarily in suspension. As turbulence decreases, the heavy minerals would be deposited before the light minerals.

Bed Forms and Hydraulic Variables

Observations of the four runs in this study and other experimental runs made in the large flume, as well as field observations, indicate that the bed configuration is the most important single factor affecting the opaque heavy mineral segregation. Bed configuration, however, is not an independent variable but is dependent on a large number of the hydraulic variables as shown by Simons and Richardson (1966, p. 13-16). Among the most important variables affecting the bed forms are the energy slope, depth of flow, physical properties of the bed material, and velocity of flow. In flume studies, flow velocity is considered to be dependent on the energy slope and depth of flow; however, in field relations velocity is the independent variable and depth of flow is probably the dependent variable.

Under the flow conditions of this study there appears to have been three fundamental types of heavy mineral segregation.

1. Thin accumulations of opaque heavy minerals covering small areas ~~that were~~ associated with dunes without the topset beds and the stoss slope of large dunes with topset beds.
2. Accumulations of opaque heavy minerals ~~that were~~ associated with the topset deposits of large dunes.
3. Accumulations of opaque heavy minerals that were associated with flat-bed movement of the sediment.

The small areas of thin accumulations of opaque heavy minerals were found in association with ripples and small dunes. On larger dunes small areas of heavy mineral accumulations formed on the dune stoss slope, commonly in the areas just downstream from the reattachment point of the flow (the location where the flow impedes on the bed after it ~~had~~ passes over the upstream dune front). The ~~areas~~ accumulations of opaque heavy minerals moved

up the stoss side of the dune as units and additional grains were added to the migrating areas during their movement. As erosion and transportation of the sediment occurred all along the stoss slope of the dune, the downstream movement of the opaque heavy mineral grains in the thin areas of accumulation is best explained by their greater resistance to movement than that of the light mineral grains. The opaque heavy mineral accumulations appeared to move slowly up the dune while the light minerals move rapidly past the heavy mineral area. Dark opaque heavy mineral accumulations generally moved as very thin ripples having very large L/H ratios (fig. 13B). Movement of such a form appears to have occurred by (1) increased scour upstream of the concentrated heavy mineral area and by (2) increase in height of the ripple build up of heavy minerals. In both situations the heavy minerals became increasingly exposed to a stronger flow conditions.

Large areas of opaque heavy mineral accumulations often were associated with topset deposits that occurred on large dunes and transition bed forms. The greatest thicknesses of dark opaque mineral accumulations were associated with this type of deposit. Three different situations associated with the topset accumulation of opaque heavy mineral grains were: (1) Accumulations that occurred along the crestal region of the dunes. These opaque heavy mineral accumulations moved downstream with the dune. If the dune maintained approximately the same shape and height, the crestal accumulation did not dissipate except for small amounts carried into suspension. These losses were offset by additions of heavy minerals from upstream areas. (2) Laminae of opaque heavy minerals that occurred downstream of the crest line were found both upon and within the topset beds. These heavy mineral deposits were derived from a crestal accumulation. (3) Foreset laminae of opaque heavy mineral grains: The segregated opaque heavy mineral laminae

in the foreset could be traced up slope in many cases into the topset beds. The foreset accumulations were caused by conditions similar to those that deposited the opaque heavy mineral laminae in the topset beds except that the heavy mineral grains were transported in sufficient quantities past the brink point to form the concentrated laminae in the foreset beds. Concentrations of opaque heavy mineral grains within laminae decreased with distance down the foreset indicating a diluting of the opaque heavy minerals with low density grains or a decrease in the proportions of opaque heavy minerals transported to that point.

The bed surface elevation of flat-bed flow under equilibrium conditions varied by only a few centimeters from a mean elevation point at any location. Conditions that produced a deep scour (in this study, a transition flow) were necessary in order to move the heavy mineral content of a thick section of the bed material near the surface before the flat-bed flow could segregate a thick accumulation of opaque heavy minerals.

During flat-bed runs, concentrations of opaque heavy minerals occurred near the base of the tractive load. This is evidenced by the widespread concentrations of opaque heavy minerals at the base of the flat beds. Other ~~concentrations~~ accumulations of opaque heavy minerals that were present within the flat-beds probably represent deposits of heavy minerals deposited in a manner similar to the way the opaque heavy mineral beds at the base of the flat beds were deposited but subsequent to deposition of the lower ~~concentrations~~ accumulations. A general absence of opaque heavy mineral grains in the suspended sediment of the flat-bed flow (table 4) indicates that the opaque heavy minerals moved as a tractive load. Results of the 20 cm flume experiment show rapid decrease with time in the ~~amount~~ volume of heavy grains transported in a flat-bed flow at near equilibrium conditions. This decrease in heavy mineral transport indicates a rapid deposition of the heavy minerals.

The location on dunes where the thickest accumulations of opaque heavy minerals occurred was the topset bed area. Runs 2 and 3 had large dunes with topset beds and large areas of thick accumulation associated with them, while dunes of run 1 had no topset beds and no large areas of concentrated heavy minerals. In order to determine why the opaque heavy minerals form the large segregations on the topset, one needs to determine how the topset deposits form. This was not a part of this study.

Topset beds were deposited with a small dip angle in the downstream direction (generally 4° to 6°) between the crest line and the brink line. In general appearance the topset beds resembled planer beds of a flat-bed run. Accumulation of opaque heavy minerals along the dune crest-line area and deposition of material forming topset beds may be due to development of the turbulent boundary layer. Differences in size between light density grains and opaque heavy minerals as well as the differences in shear stress required for movement of the two grain types are probably responsible for the preferential movement of the low density grains.

MODELS OF SYSTEMS IN WHICH OPAQUE HEAVY MINERALS ARE CONCENTRATED

Opaque Heavy Mineral Accumulations on Large Dunes

Opaque heavy minerals accumulate readily on areas of the large dunes. A slightly different concentrating mechanism seems to be important for each type of heavy mineral accumulation. However, important to each type of accumulation is the condition that larger light mineral grains are moved easier in a given flow than the smaller, more dense opaque heavy mineral grains. The greater resistance to movement of the opaque heavy minerals is shown by the relationships of relative velocities, critical shear, and the "hiding effects" of the different mineral groups.

Small thin accumulations of opaque heavy minerals form just downstream of the trough area and advance up the dune stoss slope at a rate faster than the dune movement. This occurs by:

1. Movement of grains by impinging scour just downstream of the reattachment point to a point of lower shear stress where the small thin accumulations form. Movement of the accumulation occurs because of increased resistance to the flow due to (1) increased scour upstream of the more resistant areas, and (2) the increase in thickness of the heavy mineral accumulation by the addition of heavy mineral grains from upstream. Both of the factors result in exposing the high density grains to increased flow velocity, and consequently increased local shear stress.

2. The opaque heavy mineral masses move as very thin ripples (ripples < 1 mm thick) up the stoss side of the dune back (fig. 13B), the rate of movement being primarily dependent on the amount of the opaque minerals and the temporal shear stress of the flow.

During transport up the dune the thin concentrated opaque heavy mineral mass moves to the crestal area of the dune. Segregated areas of heavy mineral grains increase in size as entrained opaque mineral grains are added from the eroded material on the dune stoss side. High on the stoss side of some dunes, these concentrations of opaque heavy grains may cover large areas (fig. 15, 18B).

An accumulation of the thin migrating opaque heavy mineral masses occurs on the high crestal region of a dune, often forming a thick deposit of the opaque heavy minerals (fig. 19B). This accumulation of opaque heavy minerals tends to migrate at a rate comparable to the rate of dune movement. In addition, the thick crestal accumulations serve as the source for the subsequent flat-bedded layers of heavy minerals in the topset. Rates of accumulation and loss of the opaque heavy minerals to

suspension and to the foreset beds, however, are variable with local hydraulic conditions.

Opaque heavy mineral grains are transported from the crestal accumulation by the unsteady stream flow. During periods of rather high turbulence and shear the opaque heavy grains are moved from the crest, transported mainly by traction, and are deposited on the topset beds (fig. 20B) downstream of the area adjacent to the crest line. During the period of high shear while the opaque heavy mineral grains are in transport, most of the light mineral grains are either carried in suspension or transported rapidly over the opaque heavy minerals by traction. With reduced turbulence and shear, subsequent deposition of light minerals buries the opaque heavy mineral layer causing it to form part of the topset bedding.

When concentrations of opaque heavy minerals are deposited just past the brink line in the foreset beds, a periodicity of transport is indicated by the alternation of light with heavy mineral layers in the foreset sequence (fig. 17A). This pattern can best be explained by intermittent conditions of strong turbulence. The intermittent turbulent eddies cause increased traction of the heavy density grains that can result in moving them past the brink point. Most of the low density material is either carried into suspension by the increased turbulence or moved rapidly over the small, high density grains.

Flat-Bed Accumulation of Opaque Heavy Minerals

A large total load is moved in the flat-bed condition and erosion and deposition occur at a rapid rate until the flow reaches near equilibrium conditions. Under equilibrium conditions the opaque heavy minerals with a higher resistance to movement than the less dense minerals, tend to move in traction at a slower rate over the bed than the light

minerals; and, therefore, the opaque heavy minerals move mainly at the base of the bed load.

Concentration of opaque heavy minerals occurs principally during slow degradation of the bed and the opaque heavy minerals concentrate at the base of the bed load. Such a situation is evidenced by numerous samples showing opaque heavy mineral accumulation directly overlying foreset beds of pre-existing bed forms (fig. 22). Deposition of the opaque heavy minerals occurs when a quasi-stablized level is reached. The opaque heavy minerals moving as bed load are buried when aggradation of the bed occurs, and the heavy mineral layer is preserved in the flat-bedded sediments.

Deposition of opaque heavy mineral beds higher in the bed is probably formed under similar conditions, except degradation does not reach the lower level of an earlier flow. Usually after the flow has reached near equilibrium conditions and flowed in that condition for some time, only small amounts of opaque heavy minerals are present at the surface. However, a short distance below the surface widespread opaque heavy mineral accumulations are present over most of the bed.

CONCLUSIONS

1. The type of bed configuration and the absence or presence of topset beds appear to be the most important factors affecting local segregation of heavy minerals in an open channel flow. Bed configuration, however, is not an independent variable but is dependent on a large number of hydraulic variables--the most important being energy slope, depth of flow, velocity of flow, and the physical properties of the bed material.

2. Three fundamental types of heavy mineral accumulations were observed in this study.

   a. Small areas of thin accumulations of opaque heavy minerals that were associated with dunes. They move as thin ripples and commonly originate in the area just downstream of the reattachment point.

   b. Accumulations of opaque heavy mineral grains that were associated with the topset deposits of large dunes. These accumulations often formed thick deposits along and adjacent to the crestal area of the dune. Opaque heavy mineral segregations were also present within the topset beds, at the surface between the crest line and brink line, and in some cases formed deposits in the foreset beds. The segregated layers in the foreset beds were probably due to mass transport of heavy minerals from the topset area past the brink line by strong conditions of turbulence.

   c. Accumulations of opaque heavy minerals that were associated with the flat-bed flows. The thickest and most widespread of the flat-bed segregations of heavy minerals occurred at the base of the flat beds, but additional laminations of heavy minerals were present in the flat beds formed by the flow.

3. Among the opaque heavy mineral sediment properties of size, gradation, and shape obtained from core samples taken from the bed, the only significant variance that occurred between runs 2, 3, and 4 was a difference in the gradation ~~coefficient~~ (σ) of the opaque heavy mineral grains.

4. Theoretical considerations indicate a distinct difference exists in the transport rates of spheres of different densities moving as bed load. There is a marked difference in initial movement of two spheres of specific gravities of 2.65 and 5.0 for theoretical bed movement. The initiation of motion of grains is illustrated by the Shields diagram (fig. 4). Based on the Shields criteria, curves can be developed that show the relationship between critical shear and grain size for materials of different densities. Two of those curves were constructed and they clearly show that the opaque heavy minerals are much more resistant to motion than the light minerals.

5. Turbulence was stronger in the trough region than on the higher portions of the stoss side or near the brink point; and, in general, the turbulence increased near the bed. The large turbulent intensity, especially as associated with the dune beds, was probably an important factor in creating large shear stresses at the bed and in moving large amounts of opaque heavy minerals on the dune stoss slopes.

6. Correlation analysis of fall velocity values for median sizes of opaque heavy mineral grains and light minerals from laminae adjacent to or within the opaque mineral laminae indicates that the median fall velocities for the two ~~grains~~ mineral groups are uncorrelated. This lack of correlation suggests fall velocity alone had little or no effect on the local sorting of heavy minerals.

7. Analyses of suspended samples from different locations in the four runs indicate that opaque heavy minerals make up less than 0.3 percent by volume of the suspended sediment. The low concentration and the size of the opaque heavy mineral grains in suspension preclude the possibility that suspension of the opaque heavy minerals is an important factor in segregation of the grains. Strong turbulent conditions may cause some local sorting of heavy minerals by the suspension or more rapid bed-load movement of the light density material.

SUGGESTIONS FOR FURTHER RESEARCH

1. This study of heavy mineral segregation was conducted with ilmenite and magnetite used as the marker minerals. Similar studies should be made using heavy minerals with distinctly different densities than those used in this study. Such research would help establish better relations of heavy mineral segregation to flow conditions, bed forms, shearing stress, and relate the fall velocity of the bed material and the heavy minerals.

2. All observations in this study have involved flow conditions and bed forms generated in a large flume. Similar conditions of heavy mineral segregation also exist in the natural environment. Segregation of dark heavy minerals has been observed by the author in streams, along the beach, along the crests of wind-blown sand dunes (Great Sand Dunes, Colorado) and in economic placer deposits (Lakehurst, New Jersey). All of these heavy mineral accumulations show similarities to the accumulations observed in the flume Studies of the transportation, deposition, and segregation of heavy minerals in the natural environment should be conducted to expand or disprove the conclusions of this study.

From the understanding of heavy mineral segregations in modern environments, the next step would be to evaluate the flow conditions and the type of sedimentation process in sandstone deposits where segregated layers of heavy minerals are preserved in the older sedimentary structures.

3. The "hiding effect," the difference in exposure to a given flow due to a difference in physical size especially between grains of different densities, may have a marked effect on the sorting of heavy minerals. Little is known about the "hiding effect" except for the general concept. By collecting and measuring the total-load samples from different sand

densities and sizes under various flow conditions in a flume, some definite conclusions should be generated about the significance of the "hiding effect."

4. Bed forms and associated bedding structures offer an important area for research. Conditions necessary for the development of topset beds on dunes and their relation to flat beds and movement of the sediment on each area of the different bed forms are in need of further study.

5. Quantitative studies of cross-bedding produced under known flow conditions would be useful in determinations of flow conditions responsible for the formation of bed forms observed in sandstones. Observations of cross-bedding in this study suggest that with decreasing Froude number for a given flow, the angle of inclination of the foreset beds produced by that flow becomes larger and the amount of variance in the foreset angle decreases.

6. Turbulence appears to be an important factor in the movement of sand grains, probably due to the increased temporal shear stress. However, only recently have techniques been developed that permit measurement of turbulence in flows containing large amounts of suspended material (Richardson and McQuivey, 1968). Studies of the intermittency of turbulence and the resulting bedding patterns due to the turbulence effect on the flow should provide new insight into sedimentary bedding patterns. Further studies such as initiated by McQuivey and Keefer (1969) could lead to a better understanding of sedimentary sorting in general as well as heavy mineral segregation.

7. Study of radio-active tracer particles of similar size and density of the material under study would help in the understanding of grain movement especially in the heavy mineral accumulations. Such a study would aid in an understanding of deposition and erosion of individual grains as well as a better understanding of the sorting processes.

APPENDIX

A. Symbols and Nomenclature

B. Grain-Mount Preparation and Relationship of Direct Grain Measurements to Sieve-Size Equivalents

C. Analyses of Opaque Heavy Mineral Grains and Light Mineral Grains from Core Samples (Runs 2, 3, 4)

D. Sediment Concentration and Size Analyses of Suspended Sediment Samples

E. Fall Velocity Values for Bed Material Sample and Core Samples from Runs 2, 3, and 4

APPENDIX A

Symbols and Nomenclature

Symbol	Definition
A	area, such as the cross sectional area of the flume
A_s	projected area of a sphere normal to particle movement
a	longest diameter for 3 mutually perpendicular axes
b	intermediate diameter of a grain for 3 mutually perpendicular axes
C_D	coefficient of drag for a sediment particle. The coefficient of drag varies with the particle geometry, relation of particle shape to flow, and the Reynolds number of the flow
C_f	coefficient of friction for a sediment particle. The coefficient of friction depends primarily on the nature of the particle surface and the surface of the material with which it is in contact.
C_L	coefficient of lift for a sediment particle. The coefficient of lift depends on the shape of the particle, relation of particle shape to flow, and the Reynolds number of the flow
c	shortest diameter of a grain with 3 mutually perpendicular axes
D	mean flow depth
d	diameter of a spherical particle
d_s	diameter of a grain--equal to sieve diameter or approximately equal to b-diameter of a particle
F_D	hydrodynamic drag force--force exerted by the flow on the particle parallel to the relative motion of the flow
F_f	frictional force--resistance to motion between two bodies in contact
F_G	gravity force
F_L	hydrodynamic lift force--the force component produced by the flow on a particle that is perpendicular to the direction of the flow and opposing the gravity force
F_N	resultant force normal to the bed surface
IF	Froude number = $U/\sqrt{gD}$ --A ratio of inertial forces to gravitational forces

Symbol	Definition
g	gravitational constant (980.7 cm/sec^2)
H	dune height--vertical distance from trough point to crest point
L	dune length--measured from trough of a given dune to trough point of the next dune upstream
n	number count of a given size in grain size analysis
Q	fluid discharge (cubic meters/sec)
q_B	bed load discharge--weight of sediment carried in bed load per unit width/unit of time
Re	Reynolds number = $\frac{UD}{\nu}$ --a ratio of inertial forces to viscous forces for the mean flow
R_*	particle Reynolds number = $U_* d/\nu$ --a ratio of inertial to viscous forces relative to a particle
R'	hydraulic radius a channel would have if the resistance to flow was limited to grain roughness (no resistance due to bed form or stream bank roughness) This term can be stated in terms of the average flow depth (D) with corrections for bed form roughness
S	energy slope of the fluid
U	fluid velocity
$\bar{U}$	mean fluid velocity
U_*	shear velocity = $\sqrt{\tau_0/\rho}$ The shear velocity is not a real velocity but is related to the real velocity which would give rise to a shear stress τ_0 (Henderson, 1966, p. 412).
$\sqrt{u^2}$	root mean square of longitudinal velocity fluctuations
V_f	velocity of flow at a representative distance from the bed
V_o	relative velocity of flow past a body
V_s	velocity of translation of a particle
V_{s_f}	velocity of a particle with a different density than the particle using V_s
W	channel width
Y	height above the bed surface

Symbol	Definition
γ	specific weight of water
γ_s	specific weight of a sediment grain
η	eddy viscosity that depends on the state of turbulent motion
ϕ	angle between the bed and horizontal line
μ	dynamic viscosity of the fluid
ν	kinematic viscosity of the fluid $=\frac{\mu}{\rho}$ —a ratio of viscosity to mass density
ρ	mass density of water
ρ_s	mass density of a particle
ρ_{s_1}	mass density of a particle with greater density than the particle with density
σ	geometric standard deviation of a sediment size distribution $=\frac{1}{2}\left(\frac{d_{84}}{d_{16}}+\frac{d_{84}}{d_{50}}\right)$
τ	shear stress in the fluid. For turbulent flow $\tau=(\mu+\eta)\frac{dU}{dY}$ and for laminar flow $\tau=\mu\frac{dU}{dY}$
τ_o	average shear stress at the bed $=\gamma DS$—force per unit area acting on the bed in the direction of flow
τ_c	critical shear stress for sediment particles—the minimum amount of shear stress necessary to start movement of particles at the bed
τ_*	dimensionless shear stress (Shields entrainment function) $=\frac{\tau_o}{(\gamma_s-\gamma)d_s}$
Φ	Einstein's intensity of bed-load transport $=\frac{q_B}{\gamma_s}\left(\frac{\gamma}{\gamma_s-\gamma}\frac{1}{gd^3}\right)$—a dimensionless measure of the bed-load transport
ψ	Einstein's intensity of shear on a particle $=\frac{\gamma_s-\gamma}{\gamma}\frac{d}{R'S}$ —a function for correlating the effect of flow with the intensity of sediment transport

APPENDIX B

Grain-Mount Preparation and Relationship of Direct Grain Measurements to Sieve-Size Equivalents

Preparation of Grain Mounts—Grain mounts for size analyses were prepared for the bed material sample, core samples and many of the suspended sediment samples studied. Where loose sample grains were used, such as the bed material sample, the sample was reduced in size by a microsplitter to a desired size. For samples of opaque heavy mineral grains and light mineral grains that were obtained from select laminations or area of a grouted core, the material was removed by use of a blunted dissecting needle. Both types of samples were prepared by distributing the grains as evenly as possible onto a petrographic slide that had previously been covered with alcohol. The grains, in settling through the alcohol, oriented themselves with their shortest axis (c-axis) perpendicular to the slide. Measurement of 500 grains for shape factor analysis showed that this orientation occurred for 88% of the grains. Those grains with the c-axis lying parallel to the slide usually had a c-axis length very similar to the intermediate axis (b-axis) length.

When the alcohol evaporated, a residue remained that caused the grain to adhere to the slide. After grain shape studies were made, Lakeside 70 and a cover glass were applied for permanent mounting and grain size measurement.

Sieve-Analysis Equivalent of Direct Measurement—Mounted mineral grains were measured directly by use of a petrographic microscope with a calibrated eyepiece that was divided into units of 12.125 microns. For most samples, intermediate axes (b-axis) were measured in unit sizes on 200 grains per slide. Where more than 200 measurements were used for a given sample, additional slides were made.

If an abundance of material was available, such as the bed-material sample, grains were selected by an equal-interval point method. A pattern of evenly spaced intervals was made by use of a modified stage micrometer mounted on the microscope. If a grain was present under the stage stop, that grain was measured. A stage interval was selected that was large enough to prevent repetition of individual grain measurements.

Slides made from samples with limited amounts of material (samples from grouted cores) were analyzed by a line measurement technique. In the line method, horizontal traverses were made over the slide at equal intervals and the b-axis was measured for each grain of the particular mineral being studied that the line crossed.

The probability of a grain being measured by the point method is in direct proportion to its projected area parallel to the slide, while the probability of a grain being "hit" by the line method is in direct proportion to the diameter of a grain perpendicular to the traverse line. Neither of these methods, however, allows for differences in the thickness of the grains perpendicular to the slide.

Opaque heavy minerals and light minerals were studied separately, and both groups had mean shape factors of near equant shape (.68 to .75 shape factor); therefore, a relation between measured size and weighted sieve equivalence was determined.

In order to make the direct measurements equivalent to the weight-size equivalents determined by sieving, a common measuring factor was used. The best common standard for such a relation was the nominal grain diameter defined as the diameter of a sphere that has the same volume as the particle (Lane, 1947, p. 937). The U. S. Inter-Agency Committee on Water Resources (1957, p. 31, 33-35) developed graphs from extensive studies that show the relation of the intermediate axes of grains

to their nominal diameters and the sieve size equivalents of grains to their nominal diameters for various shape factors. Based on the graphs of the U. S. Inter-Agency on Water Resources (1957, fig. 4, 5), the sieve diameter equivalent of the grains is .85 times the value of the direct intermediate axis measurement (using a shape factor of .7) for the grain sizes in this study.

Besides differences in b-axis and sieve-size measurement, other factors had to be considered for conversion of direct measurement to weight frequencies of a sieve analysis. Differences in grain thickness for different grain sizes had to be considered as well as the probability that a certain size grain was measured by the line method in its correct percentage proportion relative to different grain sizes. Differences in grain thicknesses were corrected by multiplying the b-size frequency count by the b-axis diameter. The probability of a grain being "hit" by the line method which is in proportion to its area parallel to the microscope stage was determined by multiplying the frequency count by the b-axis diameter. To compute a weight frequency distribution from direct measurement, the following manipulations of the direct b-axis measurements were made.

1. For the line method, the size frequency was determined by taking the percentage of each size from the sum of the sizes determined by Σnb^2

   where n is the b-axis frequency, b is the b-axis size.

2. For the area method, the size frequency was determined by taking the percentage of each size from the sum of the sizes determined by Σnb.

Cumulative curves were plotted with the weight percentages as the ordinate and with the b-axis values multiplied by .85, the correction factor, on the abscissa.

A check of the .85 conversion factor was made by using the bed-material sample. The results showed close agreement to a sieve analysis of the same material except on the large grain size end (fig. 11). Direct measurement of the b-axis of 1,000 grains showed a weighted median value of .338 mm and a gradation coefficient (σ) of 1.56. A sieved sample of the same bed material gave a median vlue of .285 mm and a gradation coefficient of 1.58. Gradation coefficients of the sieve and weighted direct measurements were similar and the difference between the two median sizes showed a value of .843, a value close to the .85 predicted by the graphs of the U. S. Inter-Agency Committee on Water Resources.

Values stated in the text of this study for a given grain-size measurement are the sieve-size equivalent values determined by the above described method and by using .85 as the size conversion factor.

APPENDIX C

Analyses of Opaque Heavy Mineral Grains and Light Mineral Grains from Core Samples (Runs 2, 3, 4)

Data on size and gradation shown for each of the samples in tables 8 and 9 were determined from direct measurement of 200 individual grains using techniques described in Appendix B. The bed-material size analyses, however, were based on 1,000 measurements.

Twenty grain measurements per sample were made for determination of mean shape factor. Shape factor as used in this report was originally defined by Corey (1949) as

$$S.F. = \frac{c}{\sqrt{ab}}$$

for three mutually perpendicular axes of the grains, where

a = maximum diameter of the grain

b = intermediate diameter of the grain

c = smallest diameter of the grain.

One advantage in the use of the Corey shape factor over other shape factors is the extensive experimental data available on sediment analysis by Schultz, Wilde and Albertson (1954) and a summarization of the work by the U. S. Inter-Agency Committee on Water Resources (1957) where the Corey shape factor was used. Discussion of the Corey shape factor as compared to other shape factors is presented by Tourtelot (1968, p. 4-7).

Measurements of the shape factor as determined for the bed-material sample of opaque heavy minerals and light minerals were each based on 60 shape factor measurements, 20 measurements on each of three grain mount slides.

For the sample identifying numbers in tables 8 and 9, the following criteria were used: Example B - 47 - B - 1
(1) (2) (3) (4)

(1) The B refers to a "bed" sample as opposed to a "S" for suspended sample (Appendix D).

(2) The 47 refers to the continuous flume experiment series run number. The following numbers are the designated run numbers for this study:

#45 = Run 1

#47 = Run 2

#48 = Run 3

#46 = Run 4

(3) The B used in the example is a selected core sample. All letters in the third position designate selected samples, while numbers indicate core samples obtained in the established sample network. Numbers and letters used are usually consecutive except for (X) used in run 2.

(4) The 1 in the fourth position designates the grain mount number made from that particular core sample.

Examples of horizontal core samples obtained from the bed including the cores from which the bed samples of light mineral and opaque heavy mineral grains were obtained are shown in figure 27.

Table 8. - Size analyses of ~~dark opaque grain mounts~~ opaque heavy minerals from core samples.

Sample	Median d_{50} (mm)	d_{16} (mm)	d_{84} (mm)	Gradation coeff. (σ)	Shape Factor	Description of Location in Bed *
Bed Material	.144	.099	.220	1.49	.684	Representative sample of Bed Material
Run 2						
B-47-B-1	.140	.098	.180	1.36	.735	Foreset, 2mm. dk. min. streak with interspersed light density min. (Sta. 86, 1.06 m right of center line)
B-47-X-1	.133	.104	.158	1.23	.747	Topset, thickest concentration in Run 2 (7mm.), dk. zone near surface (Sta. 176, 1.00 m left of center line)
B-47-36-1	.105	.083	.150	1.34	.715	Topset, dk. min. zone (0.5mm.), 3mm. below the surface (Sta. 100, .61 m right of center line)
B-47-37-1	.115	.081	.155	1.39	.711	Topset, dk. min. zone (1mm.), 1.5mm. below the surface (Sta. 96, .61 m left of center line)
B-47-46-1	.132	.103	.162	1.25	.711	Brinkpoint, dk. min. zone (1mm.), 4.5mm. below the surface (Sta. 85, .61 m left of center line)
B-47-46-2	.140	.107	.176	1.28	.718	Foreset, downstream from B-47-46-1, same dk. min. streak but with light density minerals interspersed (Sta 85, .61 m left of center line)
B-47-47-1	.112	.087	.138	1.26	.698	Topset, dk. min. zone (3mm.), 5mm. below the surface (Sta. 85, on center line)
Run 2 Ave.	.125	.095	.160	1.30	.719	
Run 3						
B-48-A-1	.126	.101	.154	1.23	.754	Topset, thickest laminae in zone, 1.5mm. thick of several thin dk. min. laminations; 5mm. from surface (Sta. 98, 1.07m right of center line).

Sample	Median d_{50} (mm)	d_{16} (mm)	d_{84} (mm)	Gradation coeff. (σ)	Shape Factor	Description of Location in Bed
Run 3 (continued)						
B-48-B-1	.154	.102	.198	1.40	.744	Topset (near Brinkpoint), dk. min. zone (1mm.) at base of topset 3mm. from surface (Sta 114, .79m left of center line)
B-48-B-2	.150	.115	.192	1.29	.769	Foreset, 2mm. dk. min. zone with interspersed light density minerals (Sta 114.2, .79m. left of center line)
B-48-10-1	.087	.063	.111	1.33	.724	Flat Bed, dk. min. zone (0.5mm.) 35mm. from the surface (Sta. 18, .61 m left of center line)
B-48-37-1	.124	.099	.161	1.28	.721	Topset, thick dk. min. zone (4mm.) at the surface (Sta 94, .61m left of center line)
B-48-40-1	.122	.088	.154	1.32	.723	Topset, uppermost dk. min. laminae (0.5mm.) in dk. min. zone 17mm. from surface (Sta. 52, .61 m left of center line)
B-48-52-1	.110	.082	.145	1.33	.751	Topset, dk. min. zone (0.5-1mm.) 4mm. below the surface (Sta. 52, .61 m left of center line)
Run 3 Ave.	.125	.093	.159	1.31	.741	
Run 4 ~~FLAT BED~~						
B-46-5-1	.144	.102	.218	1.46	.744	Dk. min. zone (1.5mm.) at base of flat-bed sands, 6mm. from surface (Sta. 176, on center line)
B-46-12-1	.100	.076	.120	1.26	.715	Dk. min. zone (1mm.) at base of flat-lying sand, 8mm. from surface (Sta 168, .61m right of center line)
B-46-20-1	.135	.095	.173	1.35	.693	Dk. min. zone (0.5mm.) interbedded w/light density, flat-lying sand, 11mm. from surface (Sta. 110, on center line)
B-46-20-2	.103	.070	.150	1.47	.748	Mixed dk. min. and lt. density minerals zone (1.5mm.) just below sample B-46-20-1. Taken 20mm. above base of flat-bed sand (Sta. 110, on center line)

Sample	Median d_{50} (mm)	d_{16} (mm)	d_{84} (mm)	Gradation coeff. ( )	Shape Factor	Description of Location in Bed
Run 4 (continued)						
B-46-26-1	.147	.095	.201	1.46	.758	Dk. min. zone (1mm.) 6.5mm. from surface, overlain and underlain by lt. density sand, 22mm. above base of flat-bedded material (Sta. 102, on center line)
B-46-52-1	.150	.082	.205	1.59	.781	Zone of dk. min. w/interspersed light density min. (1mm.), 16mm. below surface, > 35mm. above base of flat-bedded sands (Sta. 130, on center line)
B-46-55-1	.135	.086	.173	1.43	.757	Dk. min. zone w/interbedded light density grains (zone is 2.5mm. thick) at base of flat-bedded material, 15mm. from surface (Sta. 155, on centerline)
Run 4 Ave.	*.131*	*.087*	*.177*	*1.43*	*.742*	
Average of 3 Runs	*.127*	*.091*	*.165*	*1.35*	*.735*	

* Stations along the flume are designated in feet (1ft = .3048m) downstream from the headbox. (Example - the distance between Sta. 100 and Sta. 110 is 10 ft (3.05m)

Table 9. - Size analyses of light ~~density grains~~ minerals associated with ~~the dark opaque grains~~ opaque heavy minerals in the core samples

Sample	Median d_{50} (mm)	d_{16} (mm)	d_{84} (mm)	Gradation coeff. (σ)	Description of Location in Bed*
Bed Material	.287	.190	.462	1.56	Representative sample of bed material
Run 2					
B-47-B-2	.201	.150	.247	1.29	Foreset, lt. min. zone (2mm.) underlying dk. min. zone sample in B-47-B-1 (Sta. 84, 1.06 m right of centerline)
B-47-X-2	.219	.155	.276	1.33	Topset, lt. min. zone (1.5mm.) underlying dk. min. zone sampled in B-47-X-1 (Sta. 174, 100 m left of center line)
B-47-36-2	.176	.131	.244	1.37	Topset, lt. min. zone (2mm.) overlying dk. zone sampled in B-47-36-1 (Sta. 100, .61 m right of centerline)
B-47-36-3	.167	.121	.229	1.38	Topset, lt. min. zone (2mm.) underlying the dk. min. zone sampled in B-47-36-1 (Sta. 100, .61m right of center line)
B-47-37-2	.180	.136	.248	1.35	Topset, lt. min. zone (1.5mm.) underlying dk. zone sampled in B-47-37-1 (Sta. 96, .61 m left of centerline)
B-47-46-2	.222	.150	.315	1.45	Foreset below brinkpoint, lt. density grains within the dk. min. zone sampled in B-47-46-2 (Sta. 85, .61 m left of center line)
B-47-46-3	.236	.168	.349	1.44	Brinkpoint, lt. min. zone (2mm.) overlying the dk. min. zone sampled in B-47-46-2 (Sta. 85, .61 m left of center line)
B-47-47-2	.188	.138	.268	1.39	Topset, lt. min. zone (2mm.) overlying dk. min. zone sampled in B-47-47-1 (Sta. 85, on center line)
B-47-47-3	.207	.150	.266	1.33	Topset, (low angle), lt. min. zone (2mm.) underlying dk. min. zone sampled in B-47-47-1 (Sta. 85, on center line)
Run 2 Ave.	.200	.144	.271	1.37	

Sample	Median d_{50} (mm)	d_{16} (mm)	d_{84} (mm)	Gradation coeff. (σ)	Description of Location in Bed
Run 3					
B-48-A-2	.236	.170	.309	1.35	Topset, lt. min. zone (2mm.) underlying the dk. min. zone sampled in B-48-A-1 (Sta. 98, 1.07 m right of center line)
B-48-B-2	.254	.183	.343	1.37	Foreset, lt. density min. from within the zone where dk. min. were sampled in B-48-B-2 (Sta. 114, .79 m left of center line)
B-48-B-3	.290	.196	.388	1.41	Foreset, lt. min. zone (2mm.) overlying the dk. min. foreset in B-48-B-2 (Sta. 114, .79 m left of center line)
B-48-B-4	.212	.151	.280	1.36	Topset (near brinkpoint), lt. min. zone (1.5mm.) overlying the dk. min. zone sampled in B-48-B-1 (Sta. 114, .79 m left of center line)
B-48-10-2	.243	.173	.305	1.33	Flat Bed, lt. min. zone (2mm.) overlying dk. min. zone sampled in B-48-10-1 (Sta. 18, .61 m left of center line)
B-48-37-2	.199	.155	.260	1.30	Topset, lt. min. zone (2mm.) underlying dk. min. zone sampled in B-48-37-1 (Sta. 94, .61 m left of center line)
B-48-40-2	.232	.159	.299	1.37	Topset, lt. min. zone (2mm.) overlying the dk. min. zone sampled in B-48-40-1 (Sta. 94, .61 m left of center line)
B-48-52-2	.200	.141	.332	1.54	Topset, lt. min. zone (2mm.) overlying the dk. min. zone sampled in B-48-52-1 (Sta. 52, .61 m left of centerline)
B-48-52-3	.220	.169	.285	1.30	Topset, lt. min. zone (2mm.) underlying the dk. min. zone sampled in B-48-52-1 (Sta. 52, .61 m left of center line)
Run 3 Ave.	.232	.166	.311	1.37	
Run 4					
B-46-5-2	.258	.167	.360	1.47	Lt. min. zone (2mm.) overlying the dk. min. zone sampled in B-46-5-1 (Sta. 176, on center line)

Sample	Median d_{50} (mm)	d_{16} (mm)	d_{84} (mm)	Gradation coeff. (σ)	Description of Location in Bed
Run 4 (continued)					
B-46-12-2	.218	.162	.285	1.33	Lt. min. zone (2mm.) overlying the dk. min. zone sampled in B-46-12-1 (Sta 168, .61 m right of center line)
B-46-20-2	.201	.134	.286	1.46	Lt. density min. within dk. min. zone sampled in B-46-20-2 (Sta. 110, on center line)
B-46-52-1	.218	.152	.301	1.40	Lt. min. directly overlying and within the dk. min. zone sampled in B-46-52-1 (Sta. 130, on center line)
B-46-55-1	.227	.136	.362	1.63	Lt. min. zone within the zone where dk. min. were sampled (B-46-55-1). Light min. separate the v. thin dk. min. laminations (Sta. 155, on center line)
Run 4 Ave.	.224	.150	.319	1.46	
Average of 3 Runs	.218	.154	.297	1.40	

* Stations along the flume are expressed in feet (.3048 m) in a downstream direction

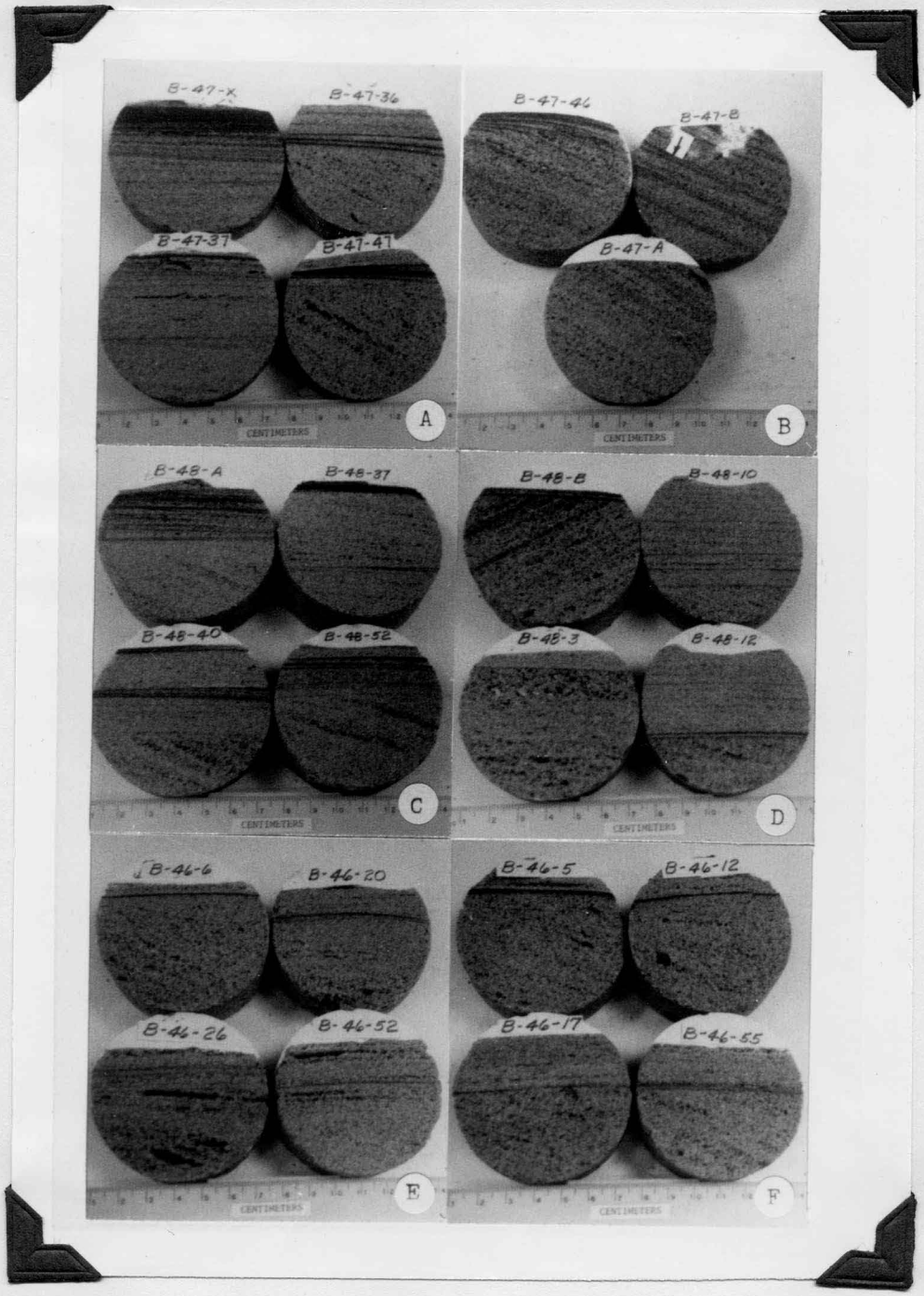

Fig. 27. Sections of core samples showing opaque heavy mineral beds in: (A) Run 2--topset beds (sample B-47-X was obtained from a crestal accumulation), (B) Run 2--foreset beds, (C) Run 3--topset beds, (D) Run 3--foreset beds (sample B-48-B) and flat bed area (samples B-48-3, 10, and 12), (E) Run 4--within the flat bed deposits, (F) Run 4--at the base of the flat beds.

Sediment Concentration and Size Analyses of Suspended Sediment Samples

Table 10. - Size analyses and concentration of suspended sediment point samples.

Run	Location	Height above bed (cm)	Conc. (ppm)	*Size (mm) d_{50}	d_{16}	d_{84}	Gradation (σ)
1	Trough	33.6	122	.146	.116	.184	1.26
		18.3	236	.186	.154	.225	1.21
		9.2	475	.172	.132	.215	1.28
		3.1	501	.172	.134	.217	1.28
	Brink point	24.4	66	.158	.127	.200	1.25
		18.3	130	.143	.108	.179	1.29
		9.2	117	.148	.116	.187	1.27
		3.1	290	.165	.128	.212	1.29
	Stoss side	18.3	291	.174	.140	.207	1.22
		9.2	234	.174	.140	.216	1.24
		3.1	343	.177	.146	.224	1.24
2	Trough	42.7	458	.138	.104	.172	1.29
		30.5	2304	.187	.146	.230	1.26
		24.4	1554	.173	.123	.209	1.31
		9.2	2022	.186	.128	.244	1.38
	Brink point	36.6	176	.127	.092	.157	1.31
		18.3	256	.138	.101	.184	1.35
		12.2	345	.140	.103	.183	1.33
		3.1	551	.145	.110	.184	1.29
	Stoss side	33.6	391	.140	.107	.176	1.28
		21.4	513	.157	.116	.205	1.33
		9.2	569	.146	.107	.190	1.33
		3.1	763	.150	.120	.188	1.25
3	Stoss side	33.6	59	.130	.102	.165	1.27
		18.3	328	.155	.117	.212	1.35
		9.2	279	.144	.112	.184	1.28
		3.1	618	.146	.115	.184	1.26
	Flat bed	27.5	25	.116	.090	.159	1.33
		21.4	39	.119	.096	.150	1.25
		12.2	218	.134	.105	.160	1.24
		7.6	974	.172	.133	.220	1.29
4	Flat bed	33.6	512	.123	.088	.156	1.33
		21.4	940	.136	.099	.168	1.30
		9.2	2103	.151	.110	.195	1.33
		3.1	6477	.183	.133	.226	1.31

*Size determined by VA tube sedimentation analysis

APPENDIX E

Fall Velocity for Bed Material Sample and Core Samples from Runs 2, 3, and 4

By use of the graph (fig. 23) constructed from data of studies conducted by the U. S. Inter-Agency Committee on Water Resources (1957), fall velocities were determined for the core samples and bed material samples (tables 8, 9). Results of these conversions from the weighted sieve equivalent sizes to fall velocity are listed in table 11.

Table 11.—Fall velocity values (cm/sec) of opaque heavy mineral grains and associated light mineral grains.

Opaque Heavy Minerals					Light Minerals				
	Fall Velocity for Size Percentile					Fall Velocity for Size Percentile			
Sample	d_{50}	d_{16}	d_{84}	Location[1]	Sample	d_{50}	d_{16}	d_{84}	Location[2]
RUN 2									
B-47-B-1	3.01	1.81	4.22	Foreset	B-47-B-2	2.59	1.74	3.36	Below
B-47-X-1	2.82	1.94	3.53	Topset	B-47-X-2	2.90	1.82	3.85	Below
B-47-36-1	1.98	1.24	3.31	Topset	B-47-36-2	2.16	1.44	3.31	Over
					B-47-36-3	2.02	1.27	3.04	Below
B-47-37-1	2.26	1.17	3.45	Topset	B-47-37-2	2.23	1.52	3.38	Below
B-47-46-1	2.80	1.90	3.64	Brinkpoint	B-47-46-3	3.15	2.02	5.00	Over
B-47-46-2	3.01	2.02	4.05	Foreset	B-47-46-2	2.95	1.74	4.46	Within
B-47-47-1	2.18	1.45	2.97	Topset	B-47-47-2	2.38	1.57	3.71	Over
					B-47-47-3	2.69	1.74	3.68	Below
RUN 3									
B-48-A-1	2.60	1.85	3.42	Topset	B-48-A-2	3.15	2.07	4.18	Below
B-48-B-1	3.42	1.87	4.76	Topset	B-48-B-4	3.78	1.76	3.94	Over
B-48-B-2	3.31	2.26	4.55	Foreset	B-48-B-2	3.48	2.28	4.67	Within
					B-48-B-3	4.03	2.50	5.62	Over
B-48-10-1	1.45	0.80	2.11	Flat Bed	B-48-10-2	3.30	2.12	4.30	Over

Table //. (continued)

Opaque Heavy Minerals					Light Minerals				
	Fall Velocity for Size Percentile					Fall Velocity for Size Percentile			
Sample	d_{50}	d_{16}	d_{84}	[1]Location	Sample	d_{50}	d_{16}	d_{84}	[2]Location
RUN 3 (continued)									
B-48-37-1	2.58	1.80	3.61	Topset	B-48-37-2	2.53	1.82	3.55	Below
B-48-40-1	2.48	1.48	3.42	Topset	B-48-40-2	3.10	1.90	4.22	Over
B-48-52-1	2.12	1.30	3.18	Topset	B-48-52-2	2.56	1.60	4.38	~~Below~~ over
					B-48-52-3	2.91	2.04	4.01	Below
RUN 4									
B-46-5-1	3.14	1.87	5.19	Base[3]	B-46-5-2	3.55	2.00	5.20	Over
B-46-12-1	1.82	1.12	2.42	Base	B-46-12-2	2.88	1.94	4.01	Over
B-46-20-1	2.85	1.65	3.98	Within[4]					
B-46-20-2	1.90	0.95	3.31	Within	B-46-20-2	2.59	1.49	4.03	Within
B-46-26-1	3.22	1.65	4.42	Within					
B-46-52-1	3.31	1.30	4.96	Within	B-46-52-1	2.09	1.78	4.13	Within
B-46-55-1	2.85	1.42	3.98	Base	B-46-55-1	3.02	1.52	5.22	Within
Bed Material	3.14	1.80	5.20	---	Bed Material	4.05	2.40	6.80	---

1. Location of laminae relative to bedding type.

2. Location of low density material relative to the sampled ~~dark~~ heavy opaque mineral laminae. The light minerals were sampled within the laminae or above or below the ~~dark~~ mineral zone.

3. In Run 4, base refers to dark mineral zone at the base of the flat-bedded sediments transported during the run.

4. In Run 4, within refers to location of sample of material taken from within the flat-bedded sediments transported during the run.

REFERENCES CITED

Allen, J. R. L., 1968, Current ripples--their relation to patterns of water and sediment motion: North-Holland Publishing Co., Amsterdam, 433p.

American Society of Civil Engineers, Task Committee on Preparation of Sedimentation Manual, 1962, Introduction and properties of sediment: Am. Soc. Civil Engineers, Proc., v. 88, no. HY4, p. 77-107.

_____, 1966, Sedimentation transportation mechanics: Initiation of motion: Am. Soc. Civil Engineers Jour., v. 92, no. HY2, p. 291-314.

American Society of Civil Engineers, Task Force on Bed Forms in Alluvial Channels, 1966, Nomenclature for bed forms in alluvial channels: Am. Soc. Civil Engineers, Proc., v. 92, no. HY3, p. 51-64.

Corey, A. T., 1949, Influence of shape on the fall velocity of sand grains: Colorado State Univ., M. S. thesis, 102p.

Daily, J. W. and Harleman, D. R. F., 1966, Fluid dynamics, Addison-Wesley Publishing Co., Reading, Mass., 454p.

Einstein, H. A., 1950, The bed load function for sediment transportation in open channel flows: U. S. Dept. Agriculture Tech. Bull. 1026, 70p.

Grigg, N. S., and Rathbun, R. E., 1969, Hydraulic equivalence of minerals with consideration of the reentrainment process in Geological Survey Research 1969: U. S. Geol. Survey Prof. Paper 650-B, p. 77-80.

Guy, H. P., Simons, D. B., and Richardson, E. V., 1966, Summary of alluvial channel data from flume experiments: U. S. Geol. Survey Prof. Paper 462-I, 96p.

Henderson, F. M., 1966, Open channel flow: The MacMillan Co., New York, 522p.

Kennedy, J. F., 1963, The mechanics of dunes and antidunes in erodible-bed channels: Fluid Mechanics Jour., v. 16, p. 521-544.

Lane, E. W., 1947, Report of the Subcommittee on Sediment Terminology: American Geophysical Union Trans., v. 28, p. 936-938.

Loyacano, J. N., 1967, Fall velocity of sand particles in turbulent flume flow: M. S. Thesis, Colorado State University, Fort Collins, Colorado, 76p.

McQuivey, R. S., and Keefer, T. N., 1969, The relation of magnetite over ripples in Geological Survey Research 1969: U. S. Geol. Survey Prof. Paper 650-D, p. 244-247.

Raudkivi, A. J., 1967, Loose boundary hydraulics: Pergamon Press, Oxford, 331p.

Richardson, E. V., and McQuivey, R. S., 1968, Measurement of turbulence in water: Am. Soc. Civil Engineers Proc., v. 94, no. HY2, p. 411-430.

Rittenhouse, G., 1943, Transportation and deposition of heavy minerals: Geol. Soc. American Bull., v. 54, p. 1725-1780.

Rubey, W. W., 1933, The size distribution of heavy minerals within a water-laid sandstone: Jour. Sed. Petrology, v. 3, p. 3-29.

Schultz, E. F., Wilde, R. H., and Albertson, M. L., 1954, Influence of shape on the fall velocity of sedimentary particles: U. S. Army Corps of Engineers, Missouri River Div., MRD Sediment Ser., no. 5, 161p.

Sears, F. W., and Zemansky, M. W., 1963, University physics, 3rd ed., pt. 1: Addison-Wesley Publishing Co., Reading, Mass., 548p.

Sheen, S. J., 1964, Turbulence over a sand ripple: M. S. thesis, University of Auckland, New Zealand.

Shields, A., 1936, Anwendung der Ahnlichkeitsmechanik und der Turbulenzforschung auf die Geschiebebewegung: Mitteilungen der Press. Versuch anst. f. Wasserbau u. Schiffbau., Berlin, no. 26, 26p.; Application of similarity principles and turbulence research to bed load movement--translated to English by W. P. Ott and J. C. van Uchelen, U. S. Dept. Agriculture, Soil Conservation Service Coop Lab., Calif. Inst. Tech., Pasadena, 21p.

Simons, D. B., and Richardson, E. V., 1963, Forms of bed roughness in alluvial channels: Am. Soc. Civil Engineers, Trans., v. 128, p. 284-302.

_____, and _____, 1966, Resistance to flow in alluvial channels: U. S. Geol. Survey Prof. Paper 422-J, 61p.

_____, _____, and Nordin, C. F., Jr., 1965, Forms generated by flow in alluvial channels: Soc. Econ. Paleontologists and Mineralogists Spec. Pub. 12, p. 34-52.

Sokal, R. R., and Rohlf, F. J., 1969, Biometry: W. H. Freeman and Co., San Francisco, 776p.

Streeter, V. L., 1966, Fluid Mechanics, 4th ed.: McGraw-Hill Book Co., New York, 705p.

Tourtelot, H. A., 1968, Hydraulic equivalence of grains of quartz and heavier minerals, and implications for the study of placers: U. S. Geol. Survey Prof. Paper 594-F, 13p.

U. S. Inter-Agency Committee on Water Resources, 1957, Some fundamentals of particle size analysis, in A study of methods used in measurement and analysis of sediment loads in streams: Washington, U. S. Govt. Printing Office, Rept. 12, 55p.

_____, 1958, Operator's manual on the visual-accumulation-tube method for sedimentation analysis of sands, Report K: St. Anthony Falls Hydraulic Laboratory, Minneapolis, Minn., 30p.